

Working efficiency of cutting tools with multilayer nano-structured Ti-TiCN-(Ti,Al)CN and Ti-TiCN-(Ti,Al,Cr)CN coatings: Analysis of cutting properties, wear mechanism and diffusion processes

Alexey A. Vereschaka, Sergey N. Grigoriev, Nikolay N. Sitnikov, Gaik V. Oganyan & Andre Batako

Abstract. The study investigated the performance properties of a carbide tool with multilayer composite nano-structured **Ti-TiCN-TiAlCN** and **Ti-TiCN-TiAlCrCN** coatings, obtained by filtered cathodic vacuum-arc deposition (FCVAD). The study considered the structure of these coatings and their basic mechanical properties (hardness, strength of adhesion bond to substrate, and elemental composition). The study included cutting tests of carbide tools with those coatings in comparison with uncoated tools and tools with reference Ti-TiN coating. The tests were carried out during the turning of steel C45 at various cutting speeds (300, 350, and 400 m/min). The study included research of the kinematics of tool wear and the nature of cracking in the structure of coatings. Diffusion processes in the system of tool substrate-coating material during machining were also studied.

Highlights

- Study of the properties and structure of Ti-TiCN-TiAlCN and Ti-TiCN-TiAlCrCN.
- Cutting tests of tools with the coatings under study at different cutting speeds.
- Mechanisms of wear and cracking in coatings.
- Diffusion processes in coated tools during cutting of metal.

Keywords: wear-resistant coatings; wear; crack; fracture; tool life; PVD coatings; diffusion.

1. Introduction

Despite the fact that wear-resistant coatings for metal-cutting tools have been actively used for more than 40 years and a large number of scientific studies have been carried out on the issue, there are still quite a lot of problems in this field to be solved. In this area, the research is developing in two main directions. New coating compositions are being developed including those involving many different elements (Ti, Al, Cr, Zr, Nb, Hf, Y, Fe, Si, Cu, B, etc.) and reagent gases (nitrides, carbides, carbonitrides, and oxides have also recently become widespread) as well as various architectures including multilayer, nano-structured, gradient, etc. On the other hand, there are new studies of the functional properties of coatings, including brittleness, plasticity, and resistance to abrasive wear, and theories and models are created to predict those properties.

A detailed review of trends and achievements in the field of research of wear-resistant coatings is given in Bouzakis et al.[1], while a survey of coating research methods is presented by Tkadletz et al.[2]. The coatings based on the systems of nitride carbides and carbonitrides of metals Ti, Al, and Cr, are most widely used.

In particular, the study of two (Ti,Al)N-based physical vapor deposited (PVD) coatings, namely, (Al,Ti)N and (Ti,Al,Cr)N, is described in the work by Fox-Rabinovich et al.[3]. In [4], Yang et al. fabricated, characterized, and evaluated nano-layered (Cr,Al,Ti)N(CrN-(Al,Ti)N) coatings with different modulation periods as well as multilayered (Cr,Al,Ti)N-(Al,Ti)N coatings with different numbers of layers and different thicknesses of individual layers. Bai et al. [5] and Lu et al. [6] studied nano-layered (Cr,Al,Ti)N coatings. Those coatings demonstrated high hardness and excellent performance in dry drilling/milling. Research described by Endrino et al. [7], Li Chen et al. [8], and Yamamoto et al. [9] studied and optimized two nano-structured coatings: (Al,Ti)N and (Ti,Al,Cr)N. The coatings AlTiN and (Ti,Al,Cr)N are commonly used as a basis for newly developed hard coatings, such as nano-composite (Veprek et al.[10]) and nano-multilayer coatings (Fox-Rabinovich et al. [11], Ning et al. [12], Yamamoto et al. [13], Yang et al. [14]).

Different mechanical properties of such coatings as (Ti,Cr,Al,Si)N[15], (Al,Cr,Ta,Ti,Zr)N [16], (Al,Si,Ti)N[17], Ti-TiN-(Ti,Cr,Al)N [18,19], Zr-(Zr,Cr)N-CrN, Ti-TiN-(Ti,Cr,Al)N [20]; Ti-(Al,Cr)N-(Ti,Al)N, Ti-(Al,Cr)N-(Ti,Cr,Al)N, Zr-(Al,Cr)N-(Zr,Cr,Al)N [21], and Zr-ZrN-(Zr,Nb,Cr,Al)N [22] were also the focus of the studies.

When Al and C are simultaneously added to the TiN system, quaternary coatings show a unique combination of both high thermal stability and outstanding tribological properties [23, 24]. The studies described in [23-29] show that the content of C plays an important role in the determination of the structure and properties of (Ti,Al)CN coatings, since C can exist in various forms. Another important factor is the content of N. The unsaturated and supersaturated contents of N result in the formation of different nitride phases and coating properties [23].

Products with nano-structured TiCN coatings, made though high temperature CVD, were described by Boehlerit GmbH & Co. [30]. Coatings of (Ti,Al)CN-(Ti,Al,Si)CN were deposited on stainless steel substrate using a four-cathode reactive direct-current unbalanced magnetron sputtering system [31]. The X-ray photoelectron spectroscopy was used to study the changes in bonding structure and chemical composition with reactive gas flow rates. The individual layers had thicknesses of 16 to 62 nm. Zeng et al. [32] report on the formation of super-hard (Ti,Al)CN coatings developed through radio frequency magnetron sputtering. The refined nano-composite structure was composed of face-centered cubic (Ti,Al)CN, hexagonal close-packed AlN crystals and amorphous carbon layers. The authors note extremely high micro-hardness of (Ti,Al)CN coatings, which reaches up to 40 GPa. Recently, multilayer nano-structured (Cr,Al)CN-CrCN coatings, deposited by combined high power impulse magnetron sputtering (HIPIMS)/ DC magnetron sputtering (DCMS), have shown considerable promise in protection of tools at elevated temperature applications [32, 33].

The studies paid much less attention to (Ti,Cr,Al)CN coatings. In particular, in [34], Majid et al. considered multilayer (Ti,Al,Si)N-(Cr,Al)N-(Ti,Al,Cr,Si)CN and (Ti,Al,Cr)CN coatings, deposited by the PVD method.

In [35], TiN co-sputtered with Cr, Al, and C were deposited on M2 steel substrates and silicon wafers by closed-field unbalanced magnetron sputtering (CFUBMS), and (Ti,Cr,Al)CN-(Ti,Al)N multilayer films were obtained. The study notes high micro-hardness of the (Ti, Al, Cr)CN coating (up to 38 GPa).

The purpose of this study was to compare the properties of two multilayer nano-structured coatings based on carbonitrides: Ti-TiCN-(Ti,Al)CN and Ti-TiCN-(Ti,Cr,Al)CN. The main mechanical properties, structure, elemental composition, and cutting properties of carbide tools with these coatings were studied during the turning of steel C45. Cutting tests of tools with these coatings were carried out in comparison with uncoated tools and with the reference coating of Ti-TiN. Moreover, the research also included the investigation of the nature of wear and failure of tools with the coatings under study and the diffusion processes occurring in tools and coatings during the cutting process.

2. Materials and Methods

2.1. Deposition method

For deposition of NMCC, a vacuum-arc VIT-2 unit was used, which was designed for the synthesis of coatings on substrates of various tool materials. The unit was equipped with an arc evaporator with filtration of vapor-ion flow, which was named filtered cathodic vacuum-arc deposition (FCVAD) in this study [36-39], and were used for deposition of coatings on tools to significantly reduce the formation of the droplet phase during the formation of coating. The use of the FCVAD process does not cause structural changes in carbide and provides:

- high adhesive strength of the coating in relation to the carbide substrate;
- control of the level of the “healing” of energy effects on surface defects in carbide in the form of microcracks and micro-pores and formation of favorable residual compressive stresses in the surface layers of the carbide material;
- formation of the nano-scale structure of the deposited coating layers (grain size and sublayer thickness) with high density due to the energy supplied to the deposited condensate and

transformation of the kinetic energy of the bombarding ions into thermal energy in local surface volumes of carbide material at an extremely high rate of about 10^{14} Ks^{-1} .

When choosing the composition of NMCC layers, forming the coating of three-layered architecture, the Hume-Rothery rule was used, which states that the difference in atomic dimensions in contacting compounds should not exceed 20% [40].

After the stage of preparing the specimen surface for bond, the supply of argon gas was cut off to make the vacuum of 10^{-7} mbar. Inert gas (argon) was supplied to the chamber to gain the pressure of 10^{-3} mbar, and then, after 10 minutes of gas ionic cleaning, an adhesive layer was deposited on Ti for 5 minutes. Then, a gas mixture (50% acetylene (ethane) C_2H_2 and 50% nitrogen N_2) was supplied to the chamber to gain the pressure of 10^{-3} mbar. In this stage, three cathodes of Al, Cr, and Ti were created simultaneously with the wear-resistant layer. The whole process took 15 minutes for the intermediate layer and 30 minutes for the wear-resistant layer. Table 1 presents the parameters used at each stage of the process of deposition of NMCC.

Table 1. Parameters of stages of the technological process of deposition of NMCC.

Process	P_{CN} (Pa)	U (V)	I_{Al} (A)	I_{Ti} (A)	$I_{Cr,}$ (A)
Pumping and heating of vacuum chamber	0.06	+20	120	65	75
Heating and cleaning of products with gaseous plasma	2.0	100DC/ 900 AC f = 10 kHz, 2:1	80	-	-
Deposition of coating	0.36	-800 DC	160	55	70
Cooling of products	0.06	-	-	-	-

Note: I_{Ti} = current of titanium cathode, I_{Al} = current of aluminum cathode, I_{Cr} -current of chromium cathode, P_{CN} = gas pressure in chamber, U = voltage on substrate.

2.2. Microstructural studies

For microstructural studies of samples of carbide with coatings, a raster electron microscope FEI Quanta 600 FEG was used. The studies of chemical composition were conducted with the use of the

same raster electron microscope. To perform X-ray microanalysis, the study used characteristic X-ray emissions resulting from electron bombardment of a sample.

The hardness (HV) of coatings was determined by measuring the indentation at low loads according to the method of Oliver and Pharr [41], which was carried out on a micro-indentometer micro-hardness tester (CSM Instruments) at a fixed load of 300 mN. The penetration depth of the indenter was monitored so that it did not exceed 10–20% of the coating thickness to limit the influence of the substrate.

The adhesion characteristics were studied on a Nanovea scratch tester, which represents a diamond cone with apex angle of 120° and radius of top curvature of 100 μm . The tests were carried out with the load linearly increasing from 0.05 N to 40 N. Crack length was 5 mm. Each sample was subjected to three trials. The obtained curves were used to determine two parameters: the first critical load, L_{C1} , at which the first cracks appeared in coating, and the second critical load, L_{C2} , which caused the total failure of the coating.

2.3. Study of cutting properties

The studies of cutting properties of a tool made of different grades of carbide with developed NMCC were conducted on a lathe CU 500 MRD in longitudinal turning of steel C45 (HB 200). The study used cutters with mechanical fastening of inserts made of carbide (WC+12% TiC+5% Co; Kirovgrad Carbide Plant–KZTS) with square shape (SNUN ISO 1832:2012) and with the following geometric parameters of the cutting part: $\gamma = -8^\circ$; $\alpha = 6^\circ$; $K = 45^\circ$; $\lambda = 0$; $R = 0.8$ mm. The study was carried out at the following cutting modes: $f = 0.2$ mm/rev; $a_p = 1.0$ mm; $v_c = 300, 350, \text{ and } 400$ mmmin⁻¹.

Flank wear land values (VB_c) were measured with toolmaker's microscope MBS-10 as the arithmetic mean of four to five tests and a value of $VB_c = 0.4$ mm was taken as failure criteria. The study included statistical processing of tests of wear of cutting tools, sample mean value of wear, and sample mean square deviation of tool wear, which are random variables with different values in repeated experiments. Furthermore, during the experiments, the outlying results were excluded. To exclude outlying results of the experiment, Irwin's criterion was used. To do that, the value of the Irwin's criterion $K\lambda$ was defined, if the outlying result is the maximum value VB_{max}

$$K_{\lambda} = (VB_c - VB_{max})/K_{\sigma}$$

and of the doubts are provoked by the wear value with minimum value VB_{min}

$$K_{\lambda} = (VB_c - VB_{min})/K_{\sigma}$$

The calculated value K_{λ} is compared to the critical value $K_{\lambda A}$, defined theoretically for a given level of significance (Level A) and selection criterion n . If $K_{\lambda} < K_{\lambda A}$, then the deviation of the questionable value of VB_c should be considered valid.

3. Results and Discussion

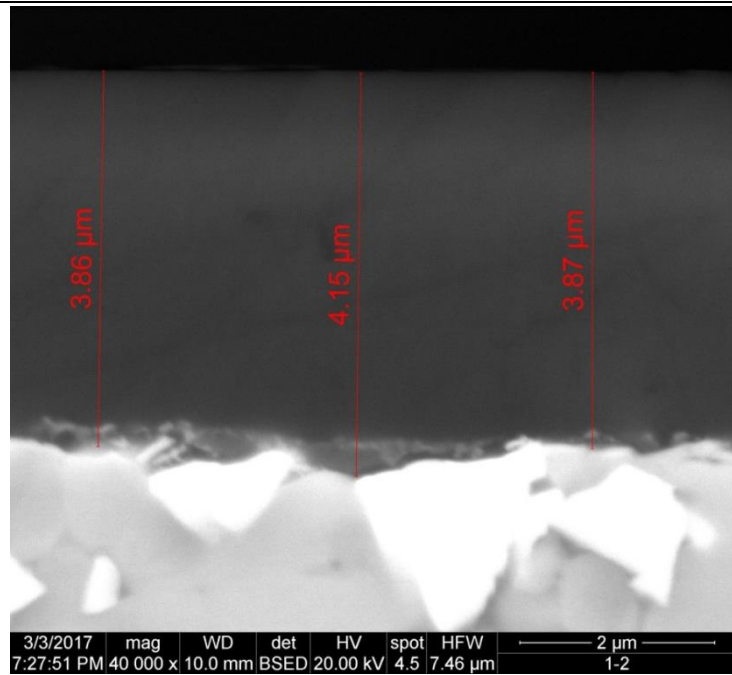
3.1. Studies of coatings microstructure and composition

Three-layered coating architecture is proposed, where the function of each of the layers is as follows.

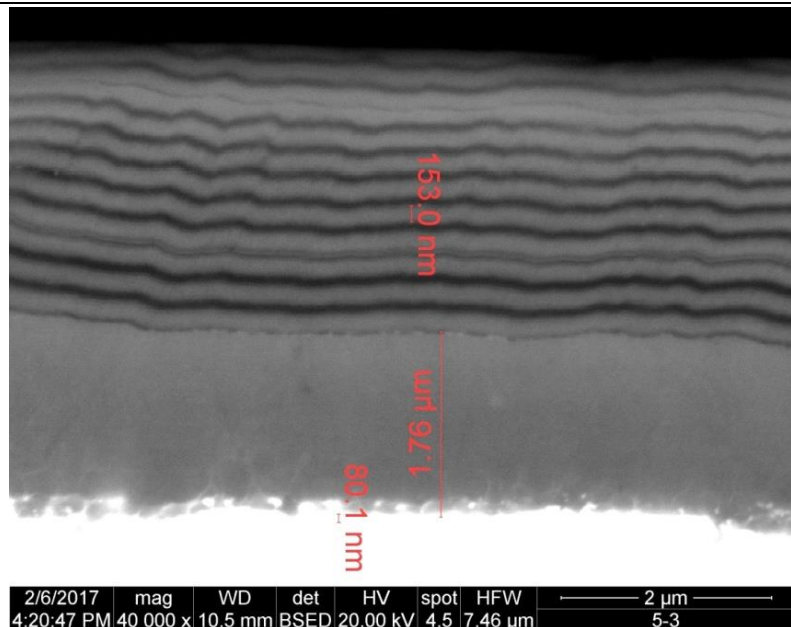
- The outer wear resistant layer at immediate contact with the material to be machined and having the major function to reduce the physical and chemical activity of the cutting tool material and to diminish adhesion with the workpiece material.
- Intermediate (transitional) layer with the primary function of supporting the working capacity of the wear resistance layer and the actualization of strong adhesion with wear resistance and adhesive layers. Moreover, the functions of Intermediate (transitional) layer may also be to lower the intensity of heat flow from frictional heat sources, blocking diffusion processes between the work and tool materials and at the same time monitoring the changes in the cutting temperature or the level of thermo-mechanical stresses arising at tool–chip and tool–work interfaces.
- Adhesive sub-layer being in direct contact with the tool material, having the primary function of providing strong adhesion between tool material and the coating [21].

The micrographs obtained on cross sections of samples with the coatings under study as well as the information on their elemental composition are presented in Fig. 1.

1. Coating Ti-TiN.
Average thickness is 4.0 μm .
Thickness of adhesive layer Ti
is 100-200 nm.



2. Coating Ti-TiCN-
(Ti,Al)CN.
Composition (At%): Ti-80%
Al-20%.
Total thickness is 5.5 μm .
Thickness of adhesive layer Ti
is 80-100 nm, transition layer
TiCN – 1.7 μm ; wear-resistant
layer (Ti,Al)CN – 3.8 μm
(23 nano-layers, thicknesses
of nano-layers are 50-
165 nm).



3. Coating Ti-TiCN-
(Ti,Al,Cr)CN
Composition (At%): Ti-44%;
Al- 18%; Cr-38%.
Total thickness is 3.8 μm .
Thickness of adhesive layer Ti
is 80-100 nm, transition layer
TiCN – 0.6 μm ; wear-resistant
layer (Ti,Al,Cr)CN – 3.2 μm
(24 nano-layers, thicknesses
of nano-layers are 50-
100 nm).

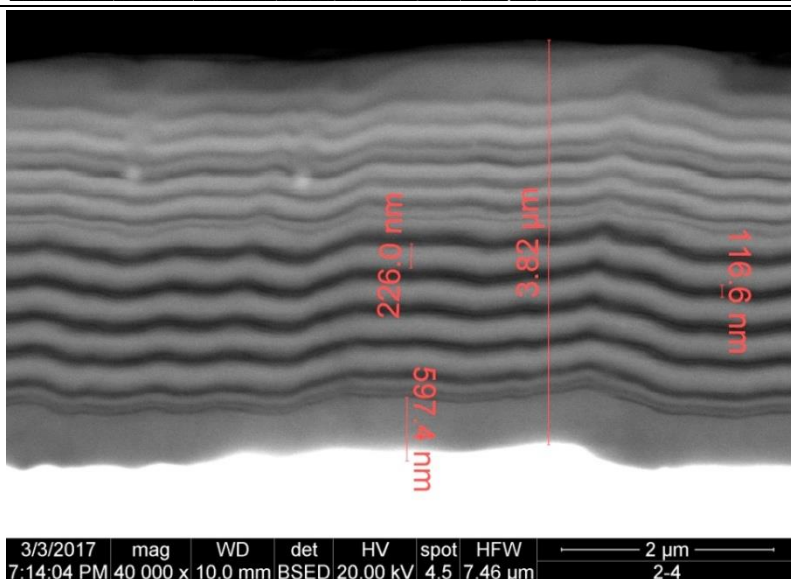


Figure 1. Microstructure of coatings of Ti-TiN (1), Ti-TiCN-(Ti,Al)CN (2), and Ti-TiCN-(Ti,Al,Cr)CN (3) on transversal cross-section.

The reference coating of Ti-TiN is of monolithic structure, without nano-layers. Coatings of Ti-TiCN-(Ti,Al)CN and Ti-TiCN-(Ti,Al,Cr)CN are of different thicknesses, mainly due to different thicknesses of the transition layer (1.7 and 0.6 μm , respectively), and these coatings have practically equal thicknesses of their wear-resistant layers (considering the possible spread of thicknesses over the surface of carbide insert $\pm 10\%$). Wear-resistant layers of coatings of Ti-TiCN-(Ti,Al)CN and Ti-TiCN-(Ti,Al,Cr)CN have pronounced nano-structures with thicknesses of nano-layers of 50-165 nm.

Let us consider individually the structure of coatings of Ti-TiCN-(Ti,Al,Cr)CN (Fig. 2(a)) and Ti-TiN (Fig. 2(b)) on the tool cutting edge. The spherical radius of the cutting edge is about 15 μm . The change of coating thickness also can be seen – from about 3.8 μm on the rake face up to about 1.5 μm on the flank face for the coating of Ti-TiCN-(Ti,Al,Cr)CN, and from 3.6 μm up to 2.7 μm for the coating of Ti-TiN. The change in thicknesses of coatings is related to the specifics of the kinematics of rotation of a workpiece during deposition of coatings.

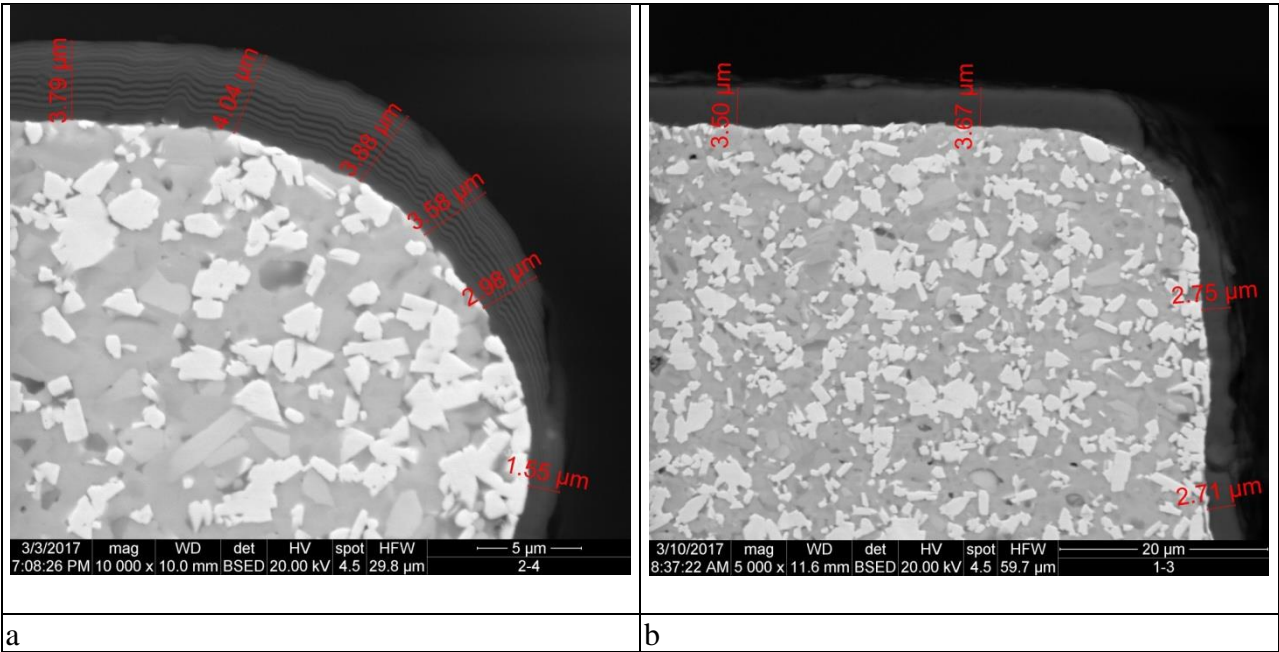


Figure 2. Microstructure of the coating of Ti-TiCN-(Ti,Al,Cr)CN (a) Ti-TiN (b) on the tool cutting edge on the transversal cross-section.

3.2. Adhesion and hardness characteristics

Table 2 presents the results of the experimental data to obtain values of L_{C1} and L_{C2} that characterize the adhesion strength of the coating with respect to the carbide substrate.

Table 2. Adhesion strength and hardness of coatings on the carbide substrate.

Structure of NMCC	L_{C1}	L_{C2}	Hardness, HV, GPa
TiN	30	36	29
Ti-TiCN-(Ti,Al)CN	-	40	37
Ti-TiCN-(Ti,Al,Cr)CN	36	39	39

From the data given, it can be concluded that the coating-substrate adhesion bonds are sufficiently strong for all coatings under study, and all three coatings are also characterized by quite high hardness.

3.3. Cutting properties studies

Curves obtained by mathematical processing of the experimental data are shown in Figs. 3, 4, 5 and 6.

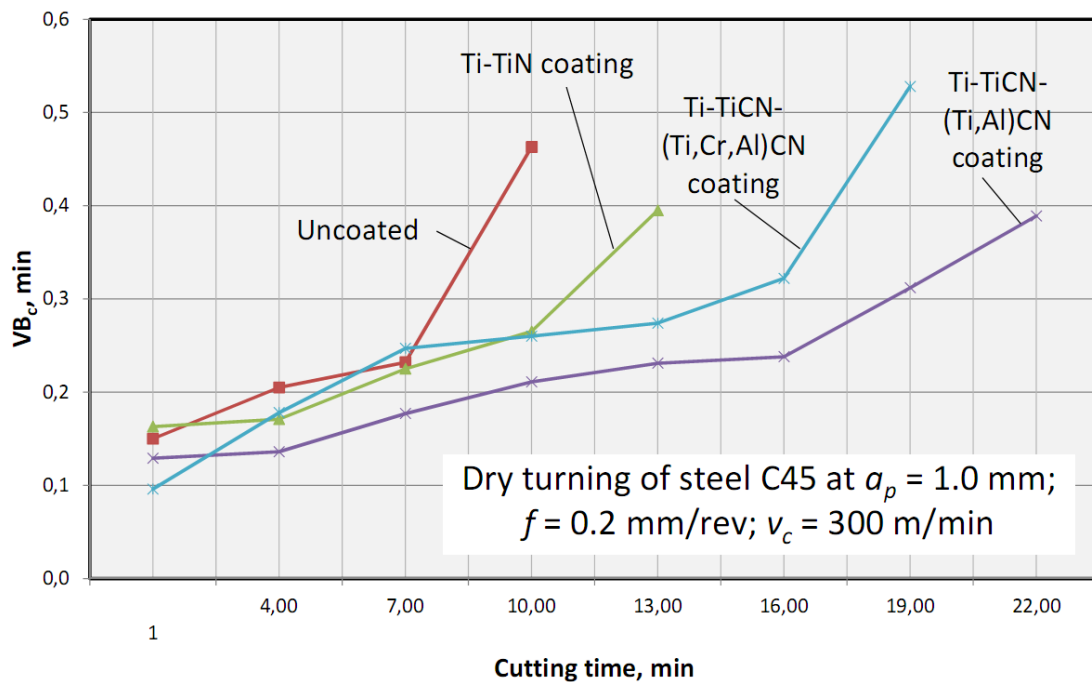


Figure 3. Dependence of wear VB on cutting time at dry turning of steel C45 $v_c = 300$ m/min.

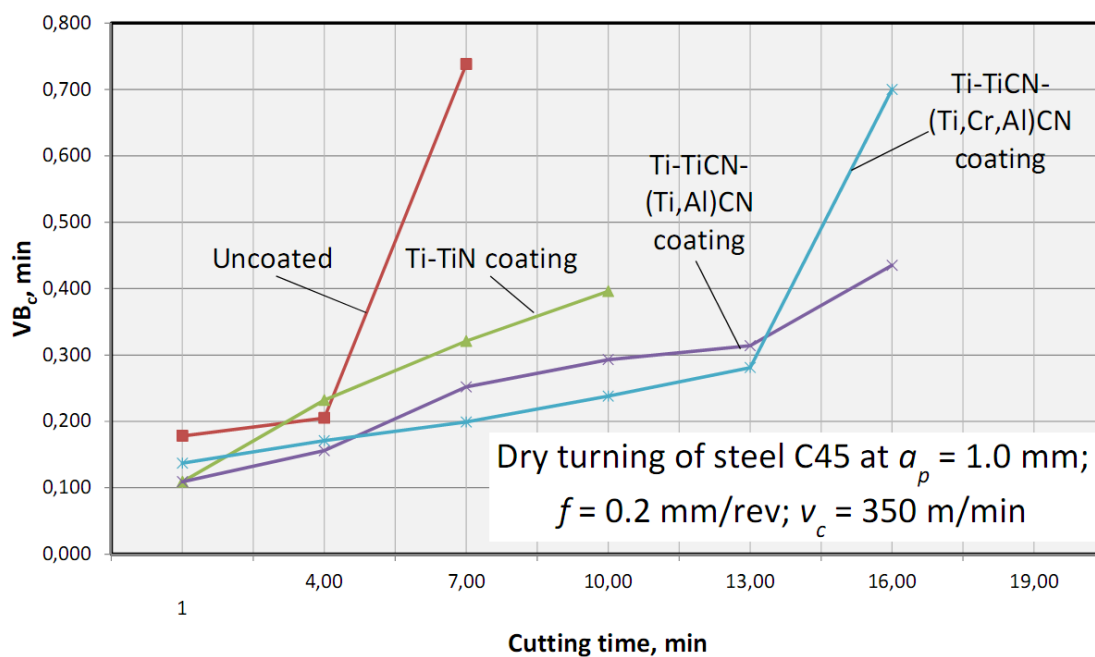


Figure 4. Dependence of wear VB on cutting time at dry turning of steel C45 at $v_c = 350$ m/min.

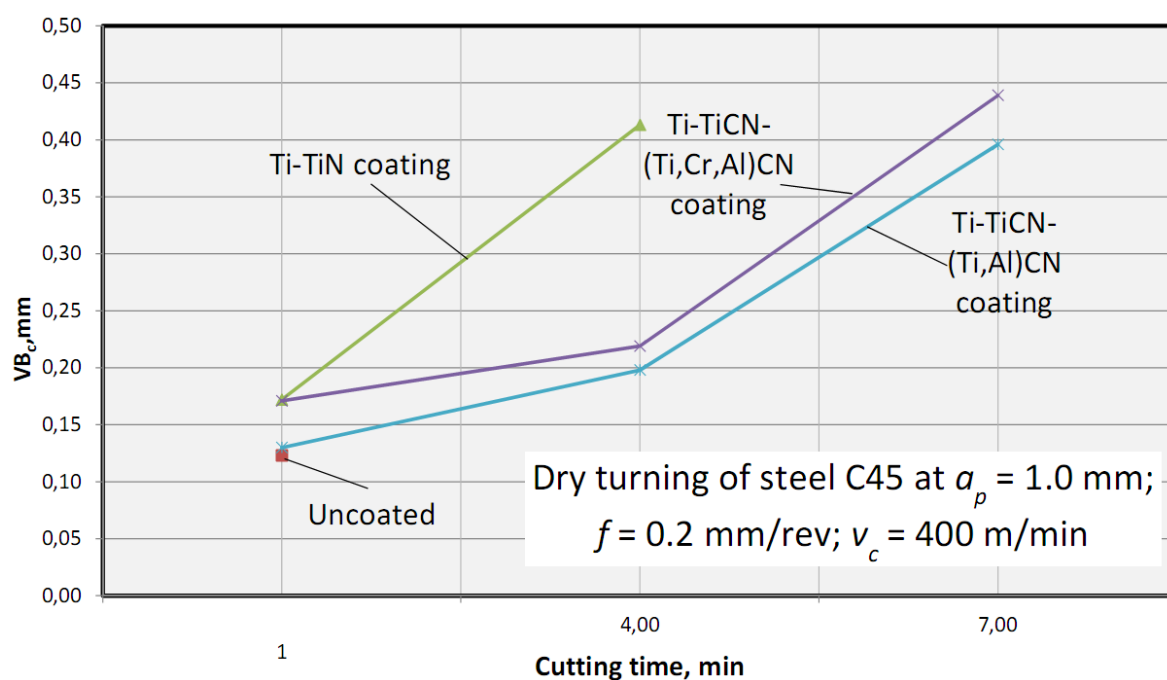


Figure 5. Dependence of wear VB on cutting time at dry turning of steel C45 at $v_c = 400$ m/min.

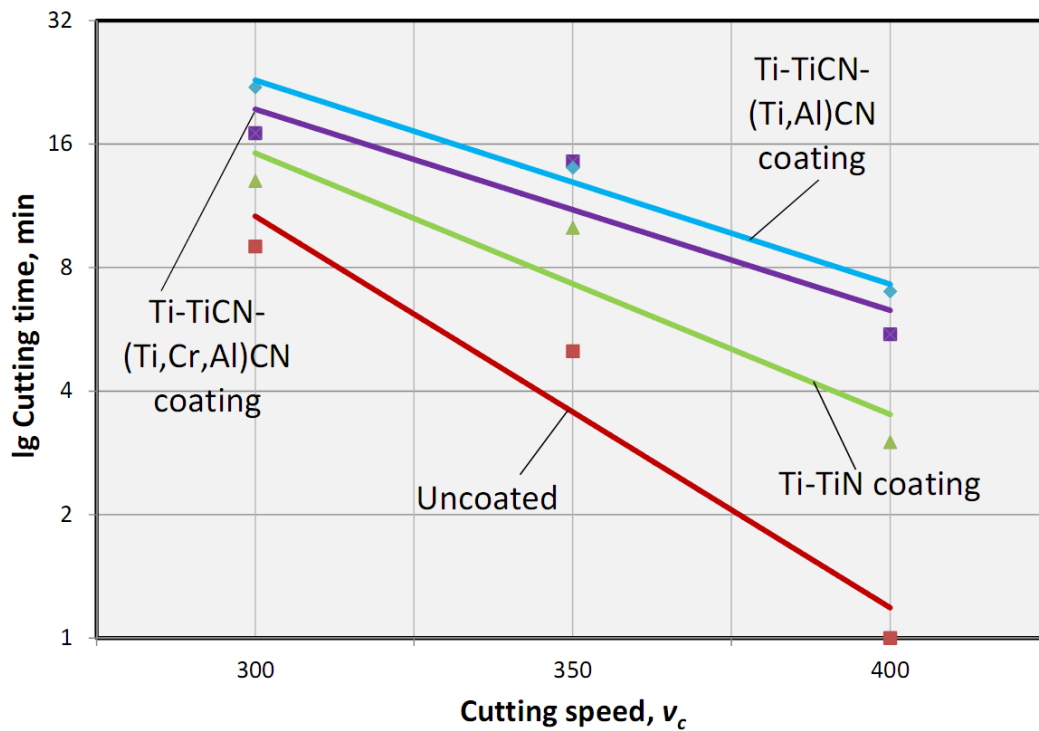


Figure 6. Dependence of cutting time on cutting speed v_c at dry turning of steel C45

Both of the carbonitride coatings under study showed markedly better wear resistance compared to uncoated tools (by 2 and 2.8 times higher at $v_c = 300$ m/min and by 2.8 to 3 times at $v_c = 350$ m/min) and tools with Ti-TiN coating (by 1.5 to 1.8 times higher at $v_c = 300$ m/min, by 1.4 to 1.6 times at $v_c = 350$ m/min, and by 1.5 to 1.8 times at $v_c = 350$ m/min). The difference in tool lives of the tools with the coatings under study, the uncoated tools and tools with Ti-TiN coatings, increases with increased cutting speed. At the cutting speed of $v_c = 400$ m/min, uncoated tools are in fact inefficient, and the tool life of such a tool is less than 3 minutes, and then catastrophic wear occurs. Meanwhile, a tool with TiN coating shows tool life of 4 minutes, with intensive wear on the flank face. Tools with coatings of Ti-TiCN-(Ti,Cr,Al)CN and Ti-TiCN-(Ti,Al)CN demonstrated a tool life of 7 minutes.

It is important to note that, in turning at $v_c = 350$ m/min, during the first 13 minutes of cutting, tools with a coating of Ti-TiCN-(Ti,Cr,Al)CN showed higher wear resistance compared to tools with a coating of Ti-TiCN-(Ti,Al)CN; however, the wear process of tools with a coating of Ti-TiCN-(Ti,Cr,Al)N was markedly intensified.

At $v_c = 300$ m/min, the significant intensification of wear of tools with a coating of Ti-TiCN-(Ti,Cr,Al)CN is observed after 16 minutes of cutting.

Meanwhile, tools with coatings of Ti-TiCN-(Ti,Al)CN showed much more stable kinematics of wear at $v_c = 300$ m/min and at $v_c = 350$ m/min. A similar picture is also observed at $v_c = 400$ m/min, when a tool with a coating of Ti-TiCN-(Ti,Cr,Al)CN showed catastrophic wear after 7 minutes of cutting, and a tool with a coating of Ti-TiCN-(Ti,Al)CN showed stable kinematics of wear, with predominant wear on the flank face after 10 minutes of cutting.

The analysis of dependence of cutting time on cutting speed v_c (Fig. 6) shows that tools with coatings of Ti-TiCN-(Ti,Cr,Al)CN and Ti-TiCN-(Ti,Al)CN demonstrated a smaller decrease in resistance with increasing cutting speed, compared to uncoated tools and tools with Ti-TiN coating.

3.4. Analysis of wear mechanisms of carbide tools with coatings under study

Various mechanisms and parameters of the wear and failure of tools are considered in detail in a number of fundamental works. In particular, it is worth noting the studies of Loladze [42, 43] and Shibasaki [44]. The problems of wear of coated tools are considered, in particular, by Vereschaka [45], Tabakov [46], Bouzakis et al. [47], and Faga et al. [48]. The problems of crack formation in coatings are considered in the works of Skordaris et al. [49] and in [50].

Study of kinematics of wear

The classic definition of wear, regardless of the cause, but here referring specifically to cutting tools, is: “the loss or dislocation of mass of a material caused by some kind of tribological phenomenon.”

Based on the data of the above studies and also based on our own data, it is possible to define two main mechanisms of wear of coated carbide tools in turning:

1. The mechanism of stable wear with predominant wear on the flank face. In this case, the flank wear land is either not formed at all or is insignificant and affects only the outer layers of the coating (Fig. 7(a)). In this case, there is flank wear land, which is the limiting wear parameter (Fig. 7(b))

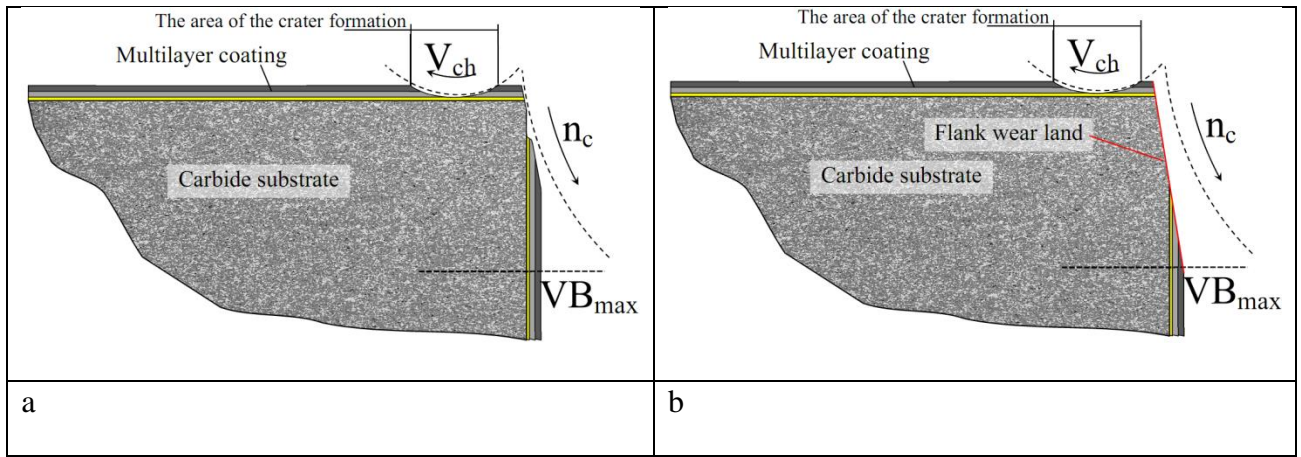
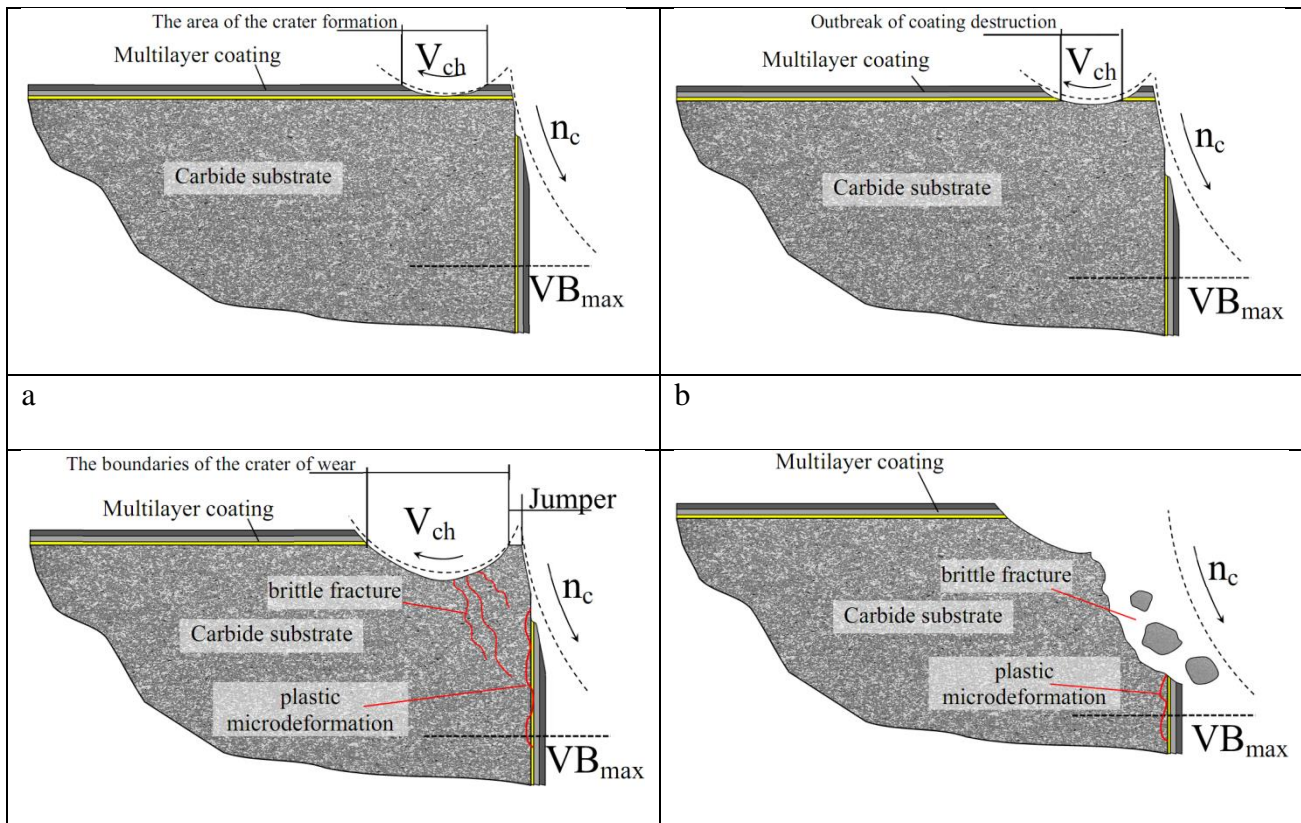


Figure 7. Pattern of wear of a coated tool with prevailing factor of wear on the flank face (V_{ch} – direction of chip movement, n_c – direction of rotation of a workpiece).

2. The mechanism that results in intensification of wear with a high risk of catastrophic wear of a tool. In this case, active formation of a wear crater on the rake face of a tool takes place, with partial destruction of the coating on the rake face of a tool (Fig. 8(b)); cracks in the substrate and coating can occur as well as a noticeable zone of plastic micro-deformation on the flank face of a tool (Fig. 8(c)). This results in plastic or brittle fracture of a jumper between a wear crater on the rake face and flank wear land and, respectively, the catastrophic wear of a tool (Fig. 8(d)).

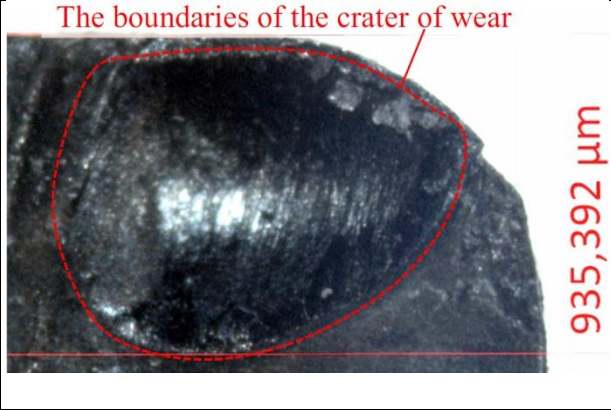
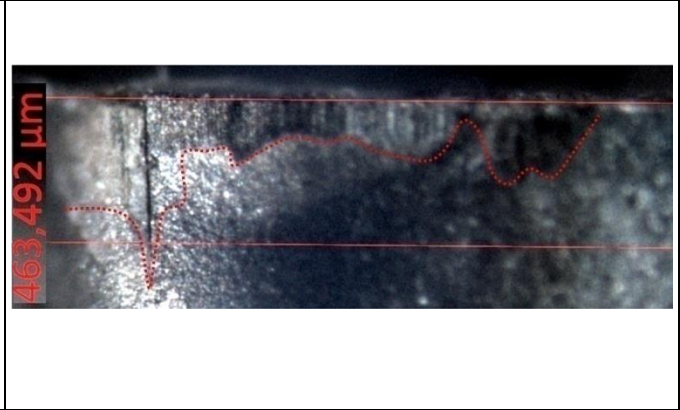
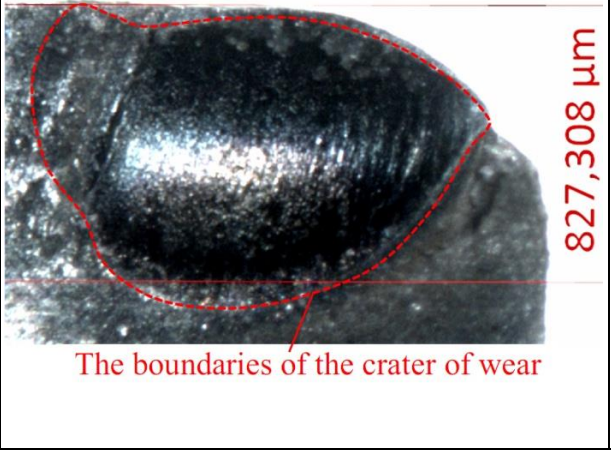



c	d
---	---

Figure 8. Pattern of wear of a coated tool with prevailing formation of a wear crater on the rake face and transition to the phase of catastrophic wear (V_{ch} – direction of chip movement, n_c – direction of rotation of a workpiece).

It is clear that the first wear mechanism is favorable since it allows good prediction of the tool life period. Accordingly, the second mechanism can be treated as unfavorable.

Let us consider the kinematics of wear of an uncoated carbide tool (Fig. 9).

	
a	b
Uncoated carbide tool. (Turning of steel C45 $f = 0.25$ mm/rev, $a_p = 1.0$ mm, $v_c = 300$ m/min), after 10 minutes of cutting. Rake face (a) and flank face (b).	
	
c	d
Uncoated carbide tool. (Turning of steel C45 $f = 0.25$ mm/rev, $a_p = 1.0$ mm, $v_c = 350$ m/min), after 4 minutes of cutting. Rake face (c) and flank face (d).	

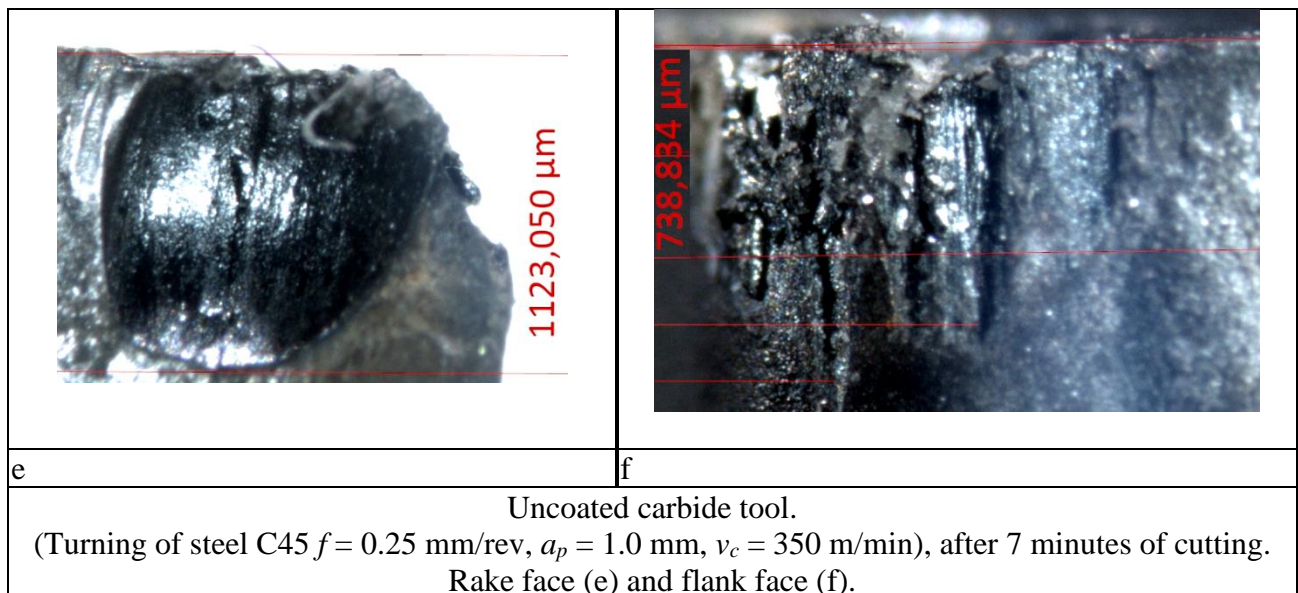
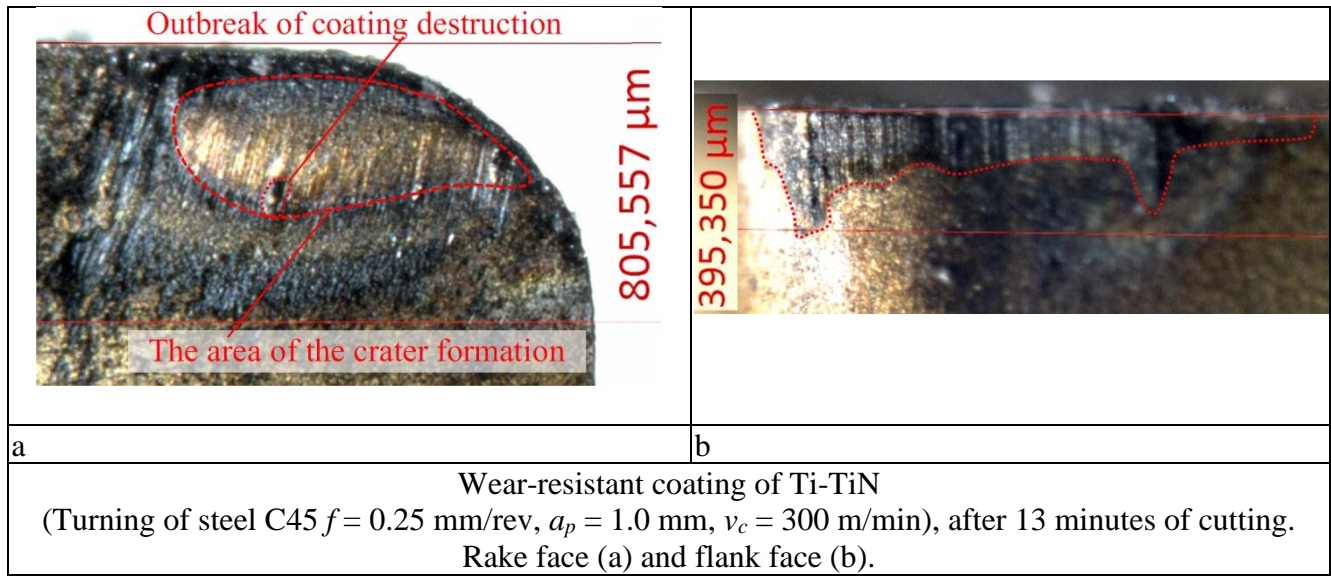


Figure 9. The final stage of wear of an uncoated tool in tuning of steel C45 at $v_c = 300$ m/min (a, b), the stage of wear, preceding catastrophic failure of a tool at $v_c = 350$ m/min (c, d), and the stage of catastrophic wear (e, f).

It should be noted that, at both cutting speeds, a large wear crater is formed on the rake face. However, at $v_c = 300$ m/min, flank wear land is a limiting wear criterion (Figs. 9(a,b)), and at $v_c = 350$ m/min, an outbreak of catastrophic wear starts, characterized by failure of tool cutting edge (Figs. 9(c-f)). At $v_c = 400$ m/min, the catastrophic wear of an uncoated tool takes place already at 3 to 4 minutes of cutting.

The pattern of wear of a tool with reference Ti-TiN coating (Fig. 10) has significant differences from the one considered earlier.



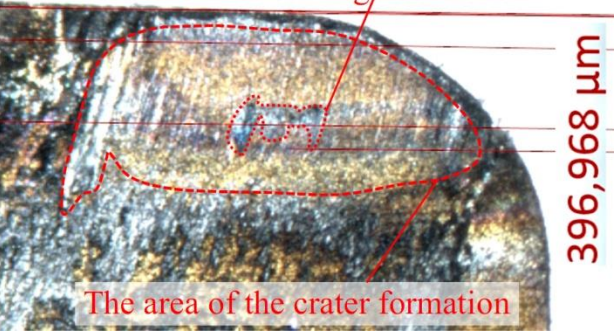
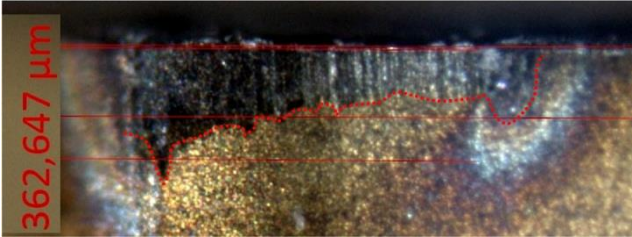
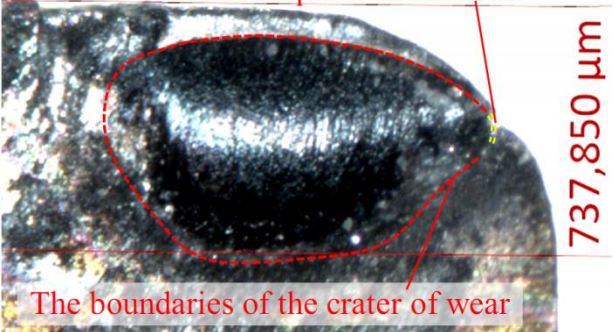
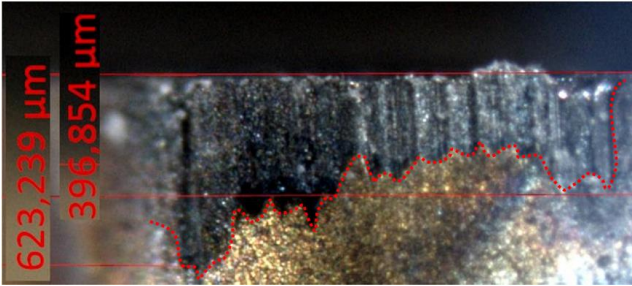
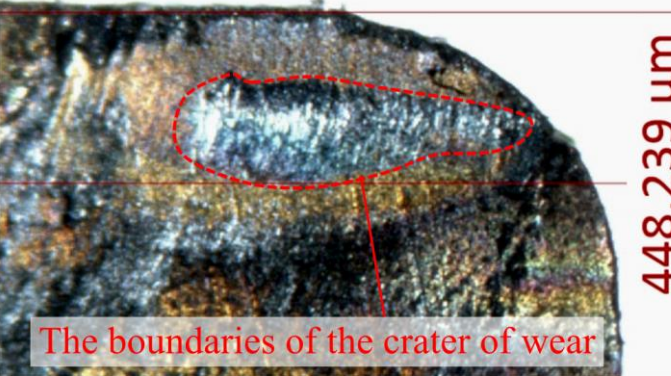
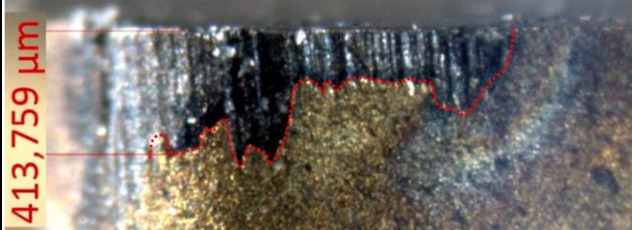
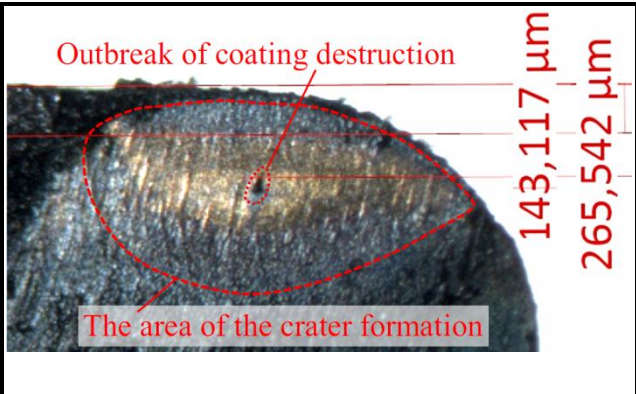
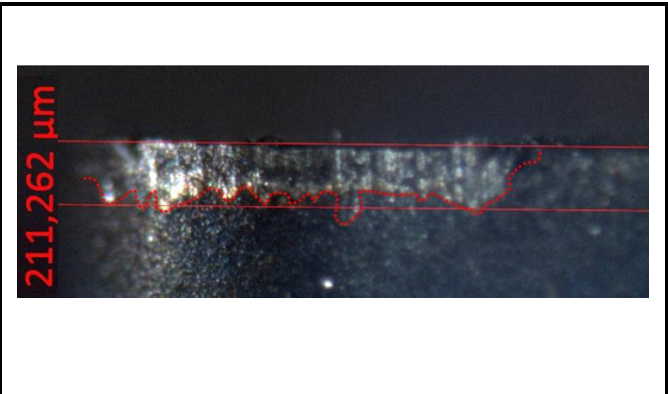
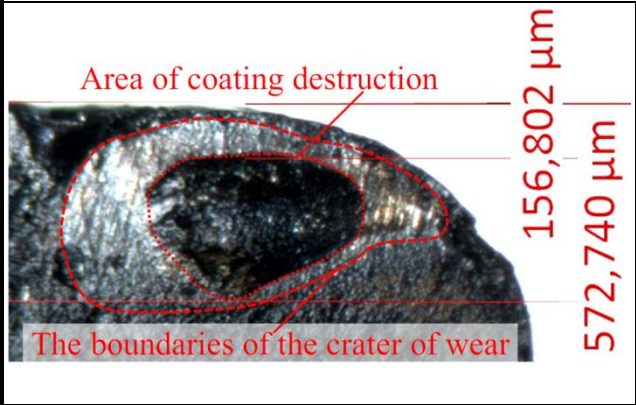
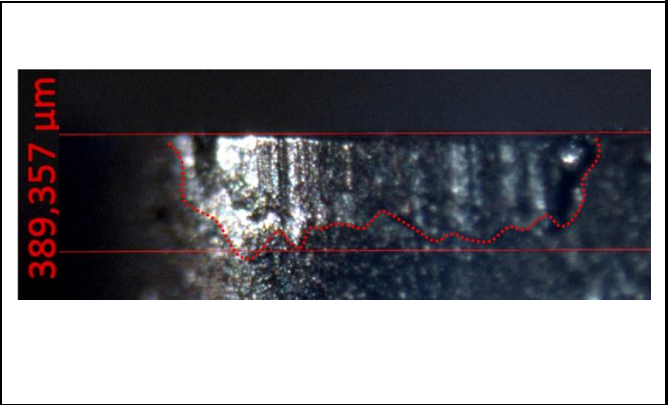
	
c	d
Wear-resistant coating of Ti-TiN (Turning of steel C45 $f = 0.25$ mm/rev, $a_p = 1.0$ mm, $v_c = 350$ m/min), after 4 minutes of cutting. Rake face (c) and flank face (d).	
	
e	f
Wear-resistant coating of Ti-TiN (Turning of steel C45 $f = 0.25$ mm/rev, $a_p = 1.0$ mm, $v_c = 350$ m/min), after 4 minutes of cutting. Rake face (e) and flank face (f).	
	
i	j
Wear-resistant coating of Ti-TiN (Turning of steel C45 $f = 0.25$ mm/rev, $a_p = 1.0$ mm, $v_c = 400$ m/min), after 4 minutes of cutting. Rake face (i) and flank face (j).	

Figure 10. Pattern of wear of a tool with coating Ti-TiN at $v_c = 300$ m/min (a, b), $v_c = 350$ m/min (c-f), and $v_c = 400$ m/min (i, j).

During cutting at $v_c = 300$ m/min, no wear crater is actually formed on the rake face, and there is only a small center of wear (Fig. 10(a)). Flank wear is a limiting wear criterion (Fig. 10(b)). At $v_c = 350$ m/min, a wear center is first formed on the rake face (Fig. 10(c)), and then a wear crater is actively formed (Fig. 10(e)), simultaneously with active wear on the flank face (Fig. 10(f)). At $v_c = 400$ m/min, only an insignificant wear crater is formed on the rake face (Fig. 10(i)); however, intensive wear on the flank face is observed (Fig. 10(j)).

Let us consider the process of tool wear with multilayer nano-structured Ti-TiCN-(Ti,Al)CN coating (Fig. 11).

	
a	b
Tool with a coating of Ti-TiCN-(Ti,Al)CN (turning of steel C45 $f = 0.25$ mm/rev, $a_p = 1.0$ mm, $v_c = 300$ m/min, after 10 minutes of cutting. Rake face (a) and flank face (b).	
	
c	d
Tool with a coating of Ti-TiCN-(Ti,Al)CN (turning of steel C45 $f = 0.25$ mm/rev, $a_p = 1.0$ mm, $v_c = 300$ m/min, after 22 minutes of cutting. Rake face (c) and flank face (d).	

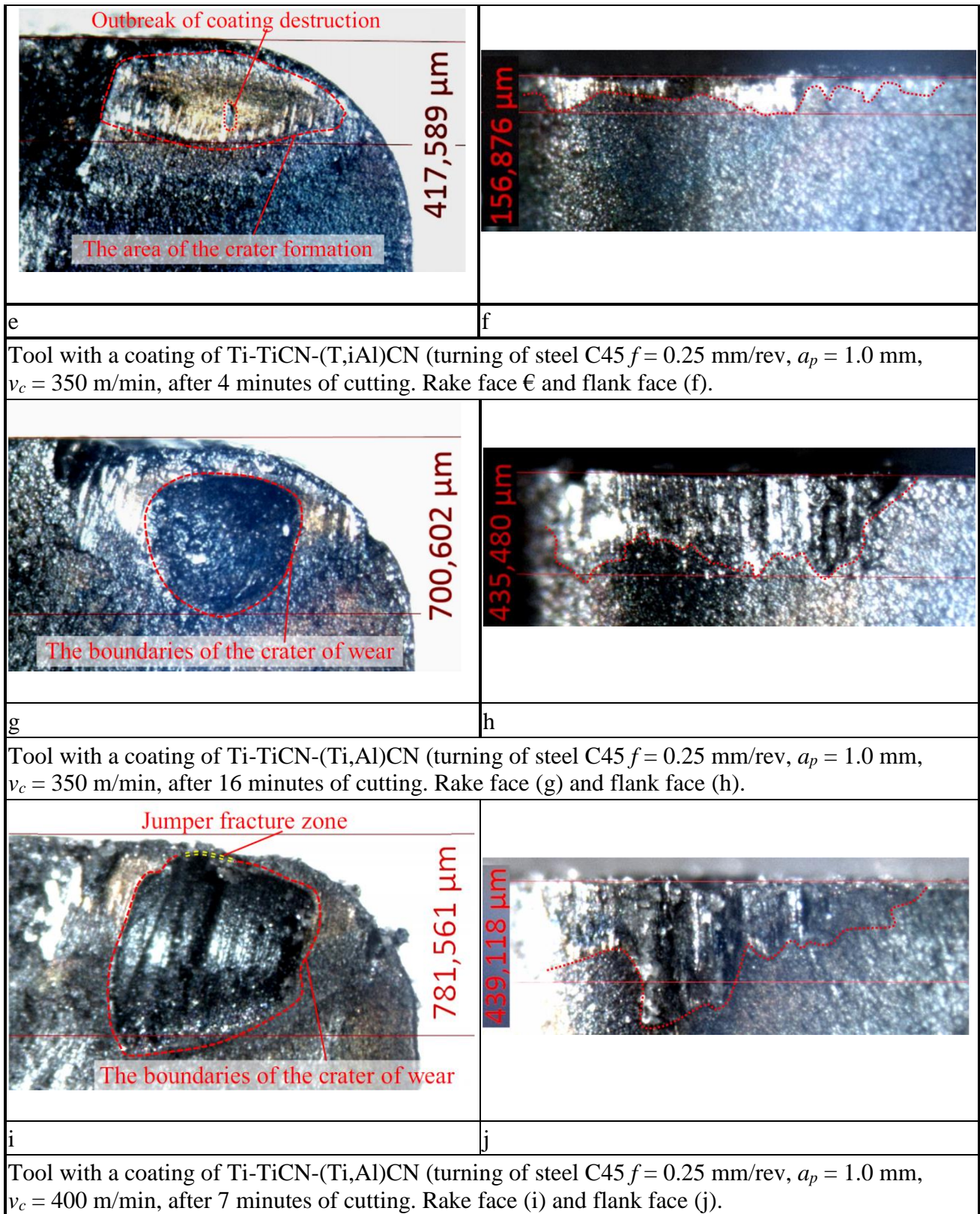


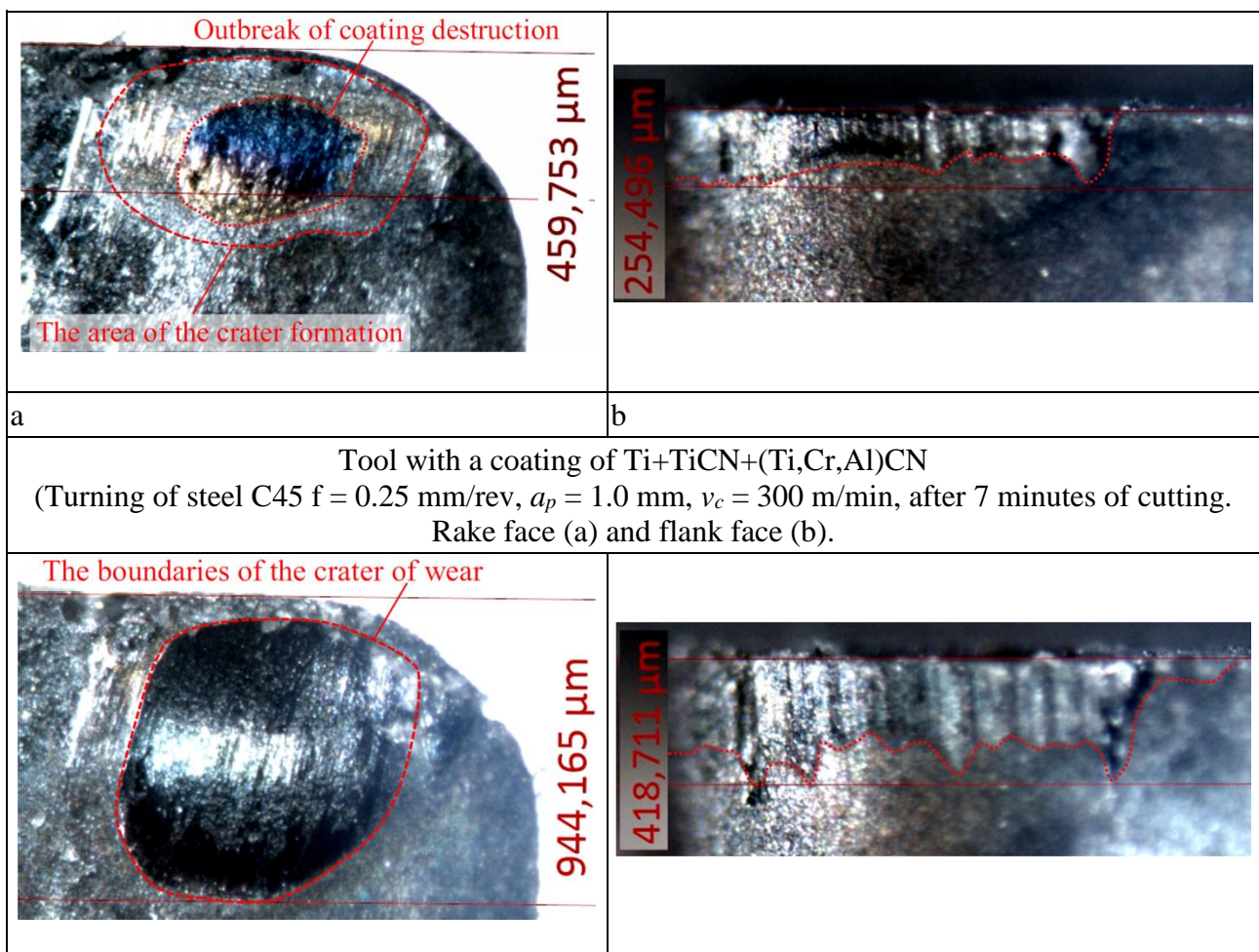
Figure 11. Pattern of wear of a tool with coating Ti-TiCN-(Ti,Al)CN at $v_c = 300$ m/min (a-d), $v_c = 350$ m/min (e-h), and $v_c = 400$ m/min (i, j).

During cutting at $v_c = 300$ m/min with a tool with a coating of Ti-TiCN-(Ti,Al)CN, a wear center is first formed on the rake face (Fig. 11(a)), and then a wear crater is formed (Fig. 11(c)). However, this

wear crater does not have a key influence on the performance of a cutting tool, and, in this case, flank wear land is a tool wear criterion (Fig. 11(d)). A similar pattern of wear, but with higher intensity, is observed at $v_c = 350$ m/min (Fig.11(e-h)). At a higher cutting speed, a wear crater on the rake face becomes more rounded, and a jump between the wear crater and the rake face decreases; however, flank wear land VB still remains a wear criterion. During turning at $v_c = 400$ m/min, a noticeable wear crater is formed on the rake face (Fig. 11(i)); however, flank wear land still remains a limiting wear criterion (Fig. 11(j)).

Let us consider the kinematics of the destruction of a tool with a coating of Ti+TiCN+(Ti,Cr,Al)CN (Fig. 12).

At $v_c = 300$ m/min, rather intensive formation of a wear crater on the rake face is observed (Fig. 12(a, c)), with sufficiently balanced wear pattern along the flank face (Fig. 12(b, d)). As a result, flank wear land remains a wear criterion at this cutting speed.



c	d
Tool with a coating of Ti+TiCN+(Ti,Cr,Al)CN (Turning of steel C45 $f = 0.25$ mm/rev, $a_p = 1.0$ mm, $v_c = 300$ m/min, after 19 minutes of cutting. Rake face (c) and flank face (d).	

Figure 12. Pattern of wear of a tool with a coating of Ti+TiCN+(Ti,Cr,Al)CN, at $v_c = 300$ m/min.

Figure 13 presents a transverse section of a wear crater, with a large visible amount of an adherent of the material being machined. The shape of the wear crater is quite symmetrical, and the depth of the wear crater is about $40\text{ }\mu\text{m}$.

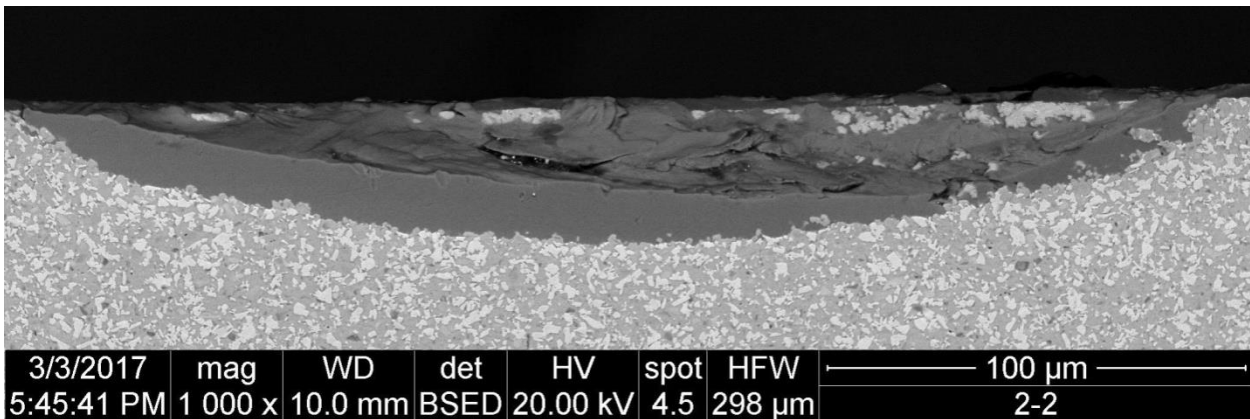
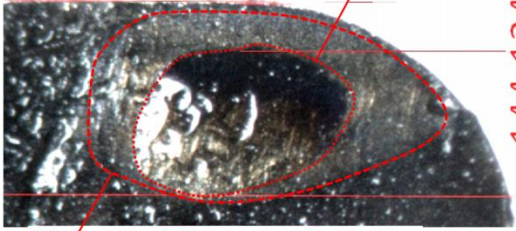
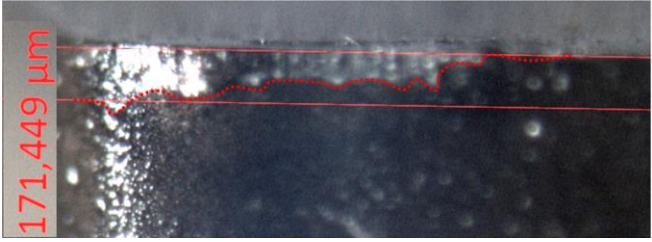
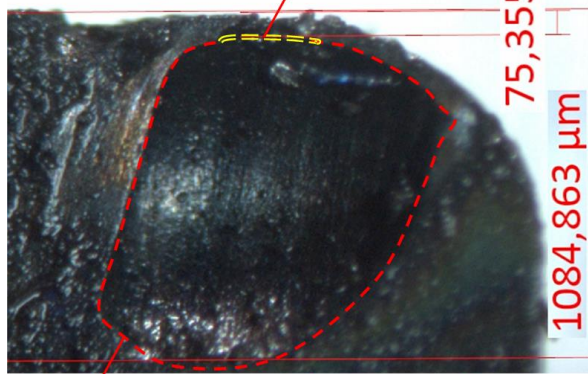
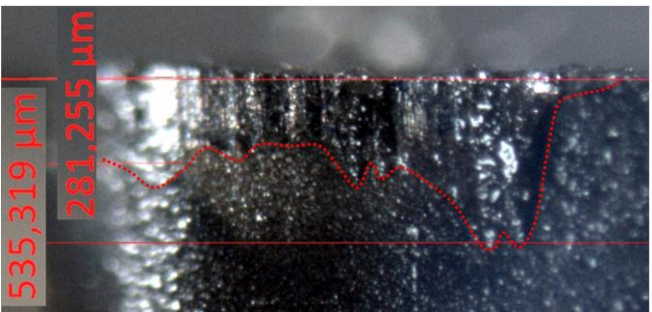


Figure 13. A wear crater on the rake face with an adherent of the material being machined. Turning with a tool with a coating of Ti-TiCN-(Ti,Cr,Al)CN at $v_c = 300$ m/min.

At $v_c = 350$ m/min (Fig. 14), a tool with a coating of Ti+TiCN+(Ti,Cr,Al)CN shows active formation of a wear crater on the rake face with relatively low dynamics of wear on the flank face. As a result, as noted above, in turning at $v_c = 350$ m/min, during the first 13 minutes of cutting, a tool with a coating of Ti-TiCN-(Ti,Cr,Al)CN showed higher resistance to wear on the flank face, as compared with a tool with coating Ti-TiCN-(Ti,Al)CN. However, by the thirteenth minute of cutting, a large wear crater was formed (Fig. 14(c)) with maintenance of the allowable flank wear value ($VB = 0.28$ mm). On the next point of the tool operation, a catastrophic wear of tool cutting edge started (Fig. 14(e, f)).

	
a	b
<p>Tool with a coating of Ti+TiCN+(Ti,Cr,Al)CN (Turning of steel C45 $f = 0.25$ mm/rev, $a_p = 1.0$ mm, $v_c = 350$ m/min, after 4 minutes of cutting. Rake face (a) and flank face (b).</p>	
	
c	d
<p>Tool with a coating of Ti+TiCN+(Ti,Cr,Al)CN (Turning of steel C45 $f = 0.25$ mm/rev, $a_p = 1.0$ mm, $v_c = 350$ m/min, after 13 minutes of cutting. Rake face (c) and flank face (d).</p>	

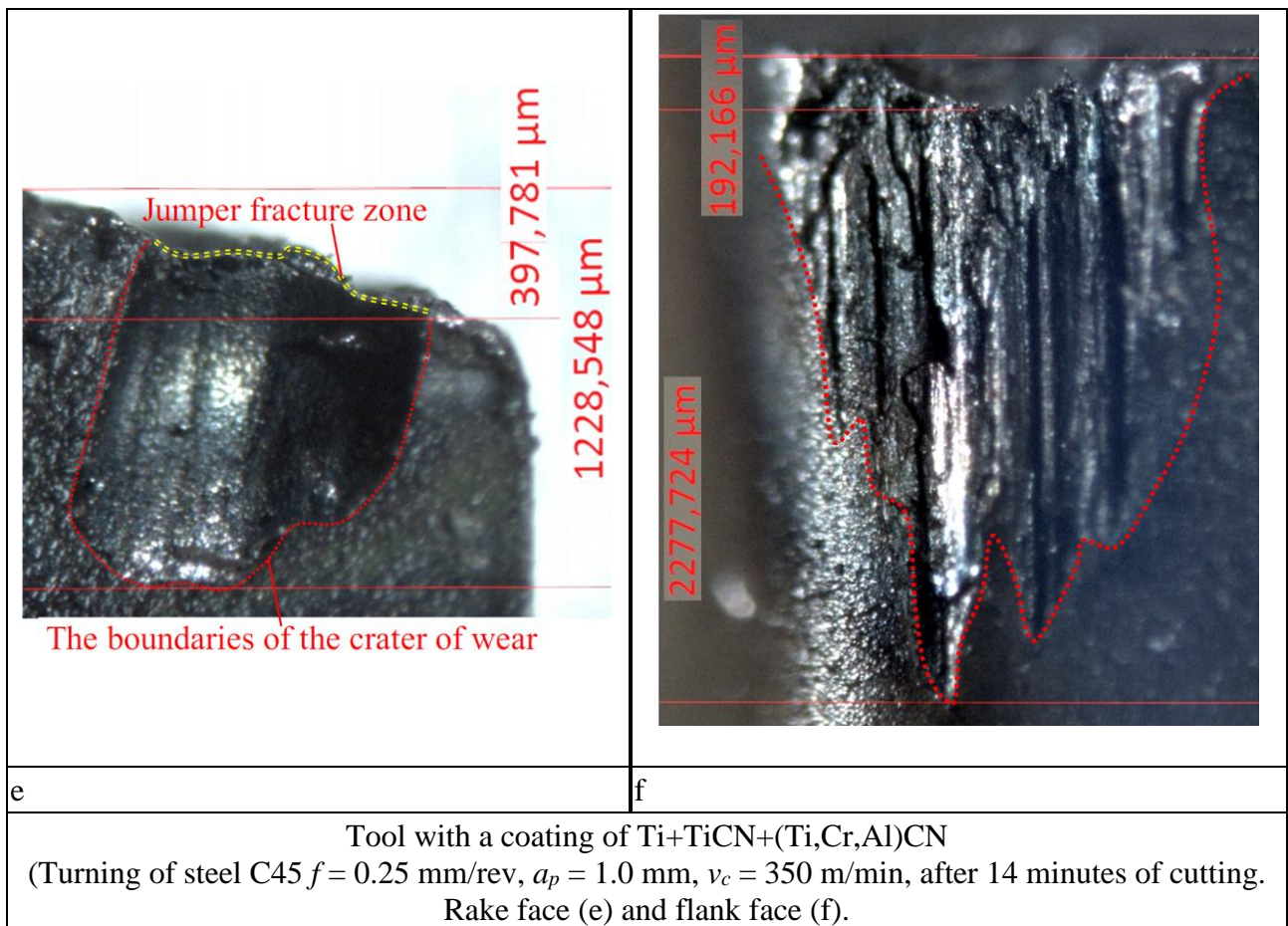


Figure 14. Pattern of wear of a tool with a coating of Ti+TiCN+(Ti,Cr,Al)CN at $v_c = 350$ m/min.

In turning at $v_c = 400$ m/min, a tool with a coating of Ti+TiCN+(Ti,Cr,Al)CN shows active wear along the rake face with formation of a large wear crater. Under this criterion, the wear is higher than that of a tool with a coating of Ti +TiCN+(Ti,Al)CN and even higher than of a tool with a coating of Ti-TiN (Fig. 15(a)). However, the wear on the flank face is significantly lower than that of a tool with a coating of Ti-TiN and slightly lower than that of a tool with a coating of Ti+TiCN+(Ti,Al)CN (Fig. 15(b)).

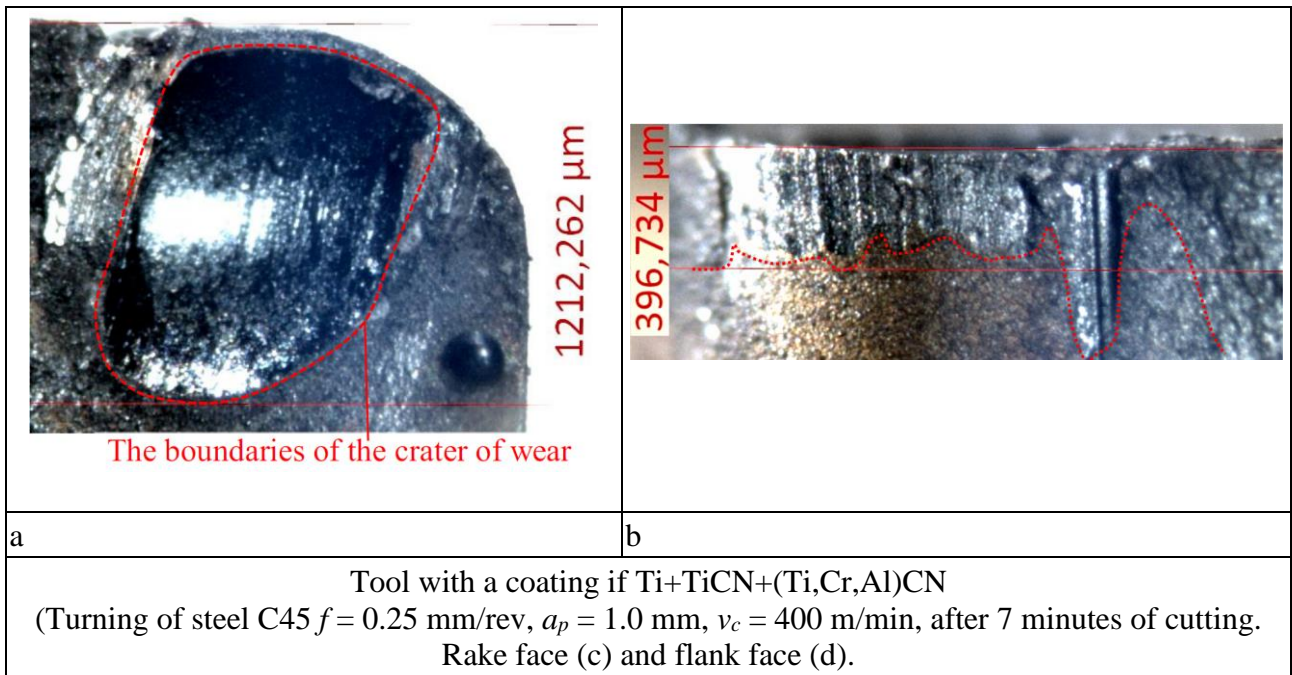


Figure 15. Pattern of wear of a tool with a coating of Ti+TiCN+(Ti,Cr,Al)CN at $v_c = 400$ m/min.

Thus, tools with coatings of Ti+TiCN+(Ti,Al)CN and Ti+TiCN+(Ti,Cr,Al)CN showed the same periods of tool life with markedly different wear patterns.

Let us individually consider the important process of cracking affecting tool life of a coated tool, usually associated [42-49] with adhesion-fatigue processes [42-49]. In particular, for a Ti-TiN coating, cracking typically occurs through formation of predominantly transverse cracks, associated with intercrystalline cracking along the boundaries of columnar crystals (Fig. 16). At the same time, in a number of cases, the formation of branching longitudinal cracks associated with intracrystalline cracking is also observed. In any case, there is a classic brittle fracture associated with the characteristics of a sufficiently brittle TiN coating and the absence of internal obstacles able to inhibit cracking.

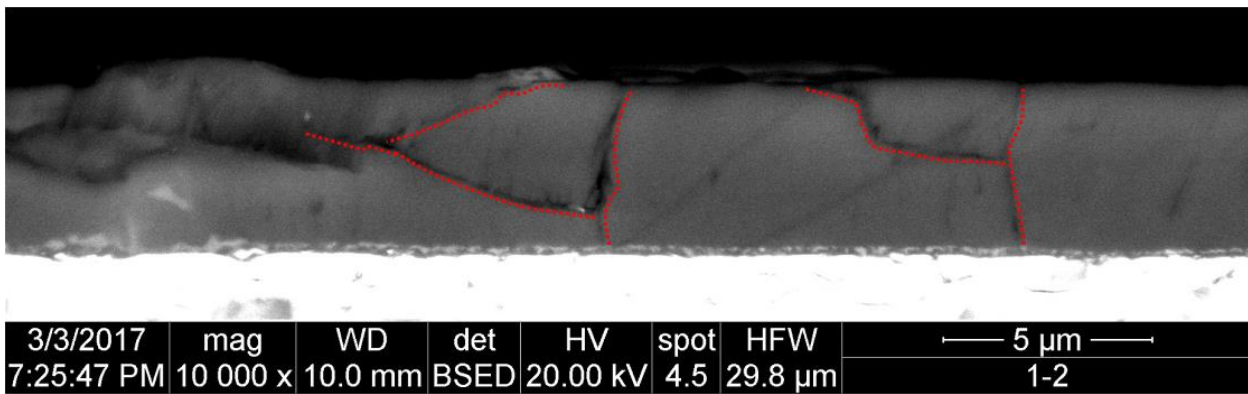


Figure 16. Nature of cracking in wear-resistant Ti-TiN coating ($v_c = 300$ m/min).

In multilayer coatings, especially in coatings with nano-layers, the nature of crack formation has significant differences [50]. By increasing the overall crack resistance of a coating, the boundaries of the nano-layers can present obstacles to the propagation of cracks. Meanwhile, weak adhesion bonds between the coating layers and cohesive bonds between the sublayers can result in the formation of delamination and longitudinal cracks. In particular, Fig. 16 shows a transverse section of a carbide tool with coating Ti-TiCN-(Ti,Al)CN. It also shows a build-up of the material being machined and a series of local delaminations between nano-sublayers of the wear-resistant coating layer. At the same time, there is a longitudinal crack in the coating structure that forms a chipping fragment of the coating.

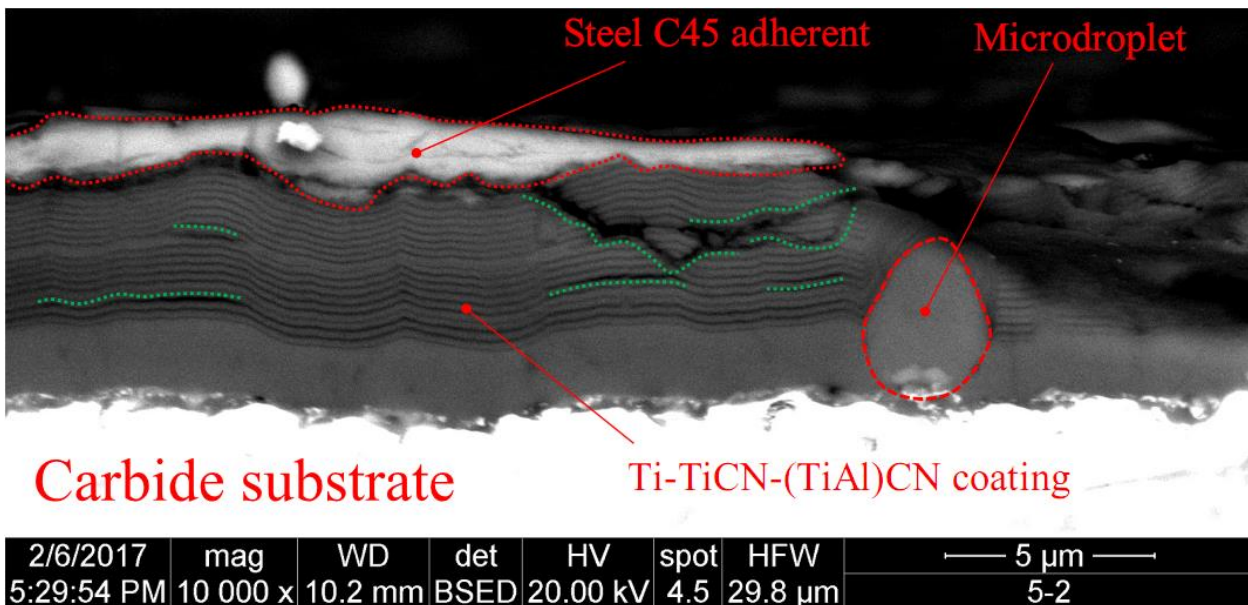


Figure 17. Nature of cracking in wear-resistant Ti-TiCN-(Ti,Al)CN coating ($v_c = 350$ m/min).

A similar picture is observed in Fig. 18. In this case, local delaminations are associated with local thickening (possibly, a “smoothed” microdroplet) in the intermediate layer of the coating. Like in the previous case, these local delaminations do not pose a serious threat to the integrity of the coating. Meanwhile, there is an extended longitudinal crack on the image. In the structure of this crack, delaminations are combined with transverse ruptures of nano-layers of the coating, and that results in peculiar “stepped” shape of crack walls. Because of insufficiently high plasticity of the compound (Ti,Al)CN, this coating shows no formation of “bridges” that prevent the development of a crack, which is typical, in particular, for nano-structured coatings based on the (Zr,Al)N system [50].

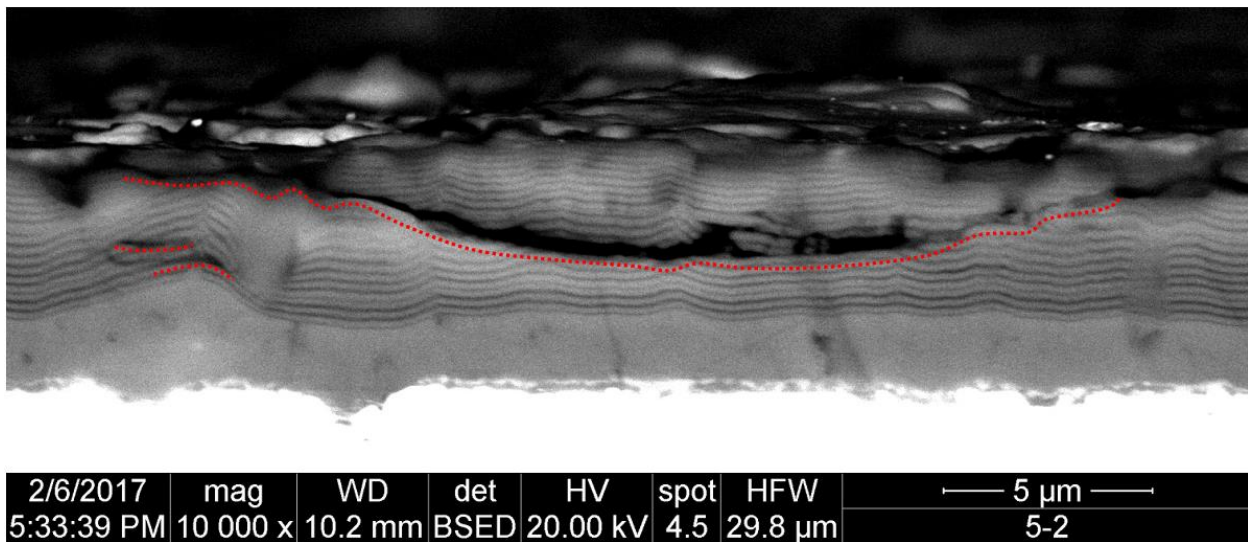


Figure 18. Nature of cracking in wear-resistant coating Ti-TiCN-(Ti,Al)CN ($v_c = 350$ m/min).

The flank face is characterized by the development of plastic micro-deformations that form a “wavy” structure of the substrate surface. Figure 19 shows an edge of a coating retaining a good adhesion bond to the substrate. In this case, a build-up of the material being machined is charged between the coating and the substrate, thus creating an appropriate tearing force.

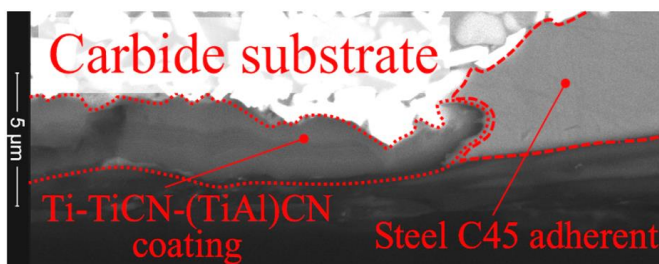
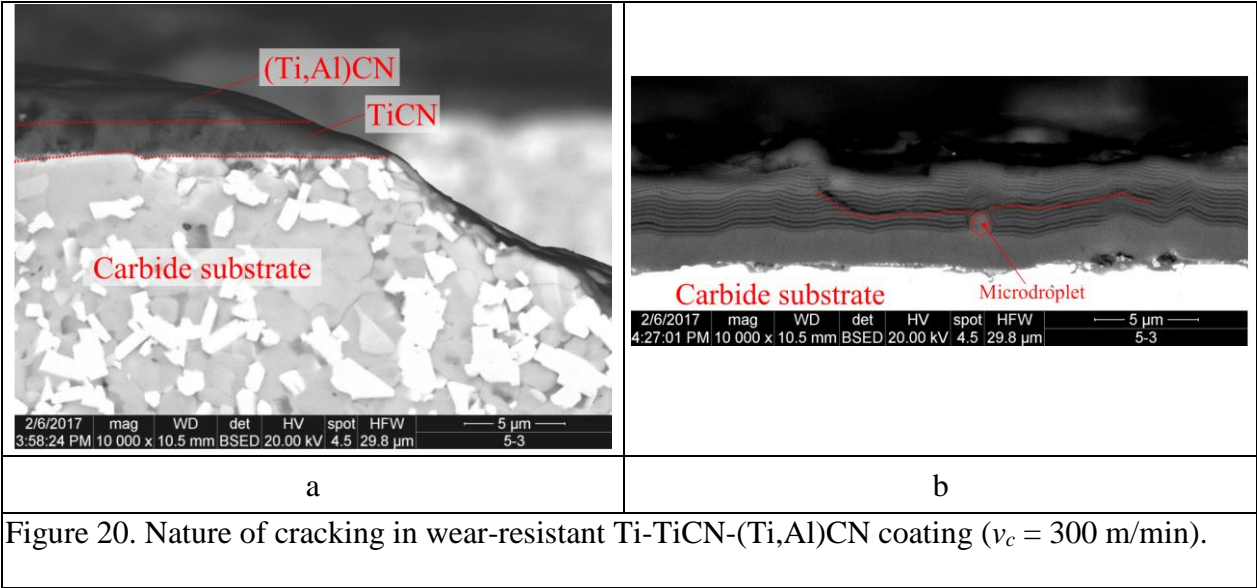


Figure 19. Nature of cracking in a wear-resistant Ti-TiCN-(Ti,Al)CN coating ($v_c = 350$ m/min) (in the flank face)

In general, the Ti-TiCN-(Ti,Al)CN coating shows good crack resistance, and that can be seen at the boundary of a remaining part of the coating in the section adjacent to wear crater (Fig. 20.a). The coating retained good adhesion to the substrate, the wear mechanism is fairly balanced, and there are no noticeable cracks in the given section.



A typical mechanism of cracking for a given coating is in formation of longitudinal cracks and local delaminations. Various internal defects of the coating, in particular, microdroplets, are a kind of a peculiar “catalysts” for the development of cracks (Fig. 20.b).

During the consideration of cracking in the Ti-TiCN-(Ti,Cr,Al)CN coating, characterized by higher hardness and, respectively, lower plasticity in comparison with the Ti-TiCN-(Ti,Al)CN coating, the following can be noticed.

This coating is also characterized by the formation of longitudinal cracks and delaminations, but these cracks are much more brittle in nature, and they often have further development in the structure of the substrate (Figs. 21, 22.a). Complete destruction of the local parts of the coating can be often observed (Fig. 22.a).

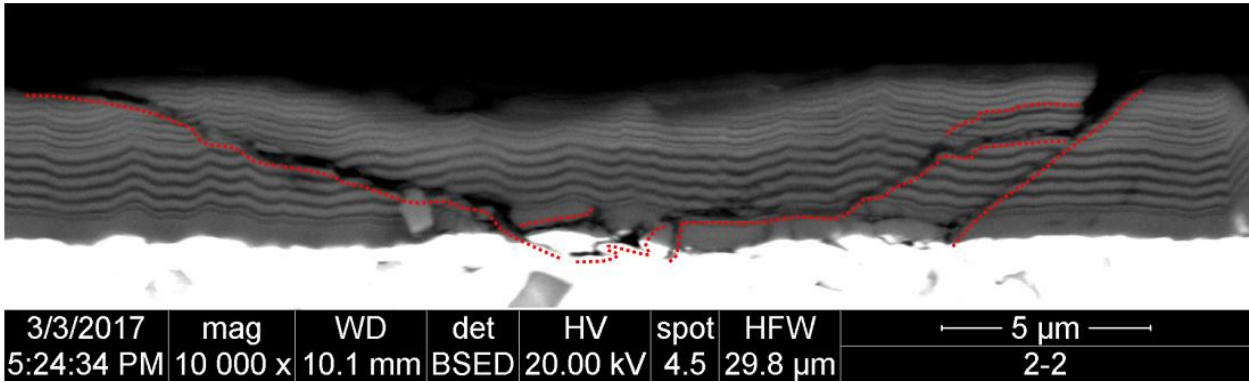


Figure 21. Nature of cracking in wear-resistant Ti-TiCN-(Ti,Cr,Al)CN coating ($v_c = 300$ m/min).

The brittle mechanism of destruction of the coating fragments is manifested in the formation of a network of longitudinal and transverse cracks with chipping of the coating fragments (Fig. 22.b). During the consideration of the nature of destruction of a coating at the boundary of a wear crater on the rake face, it is possible to notice a network of numerous microcracks, both longitudinal and transverse ones (Fig. 22.c). This area has a significant difference from a similar region of fracture of a tool with Ti-TiCN-(Ti,Al)CN coating (see Fig. 20.a).

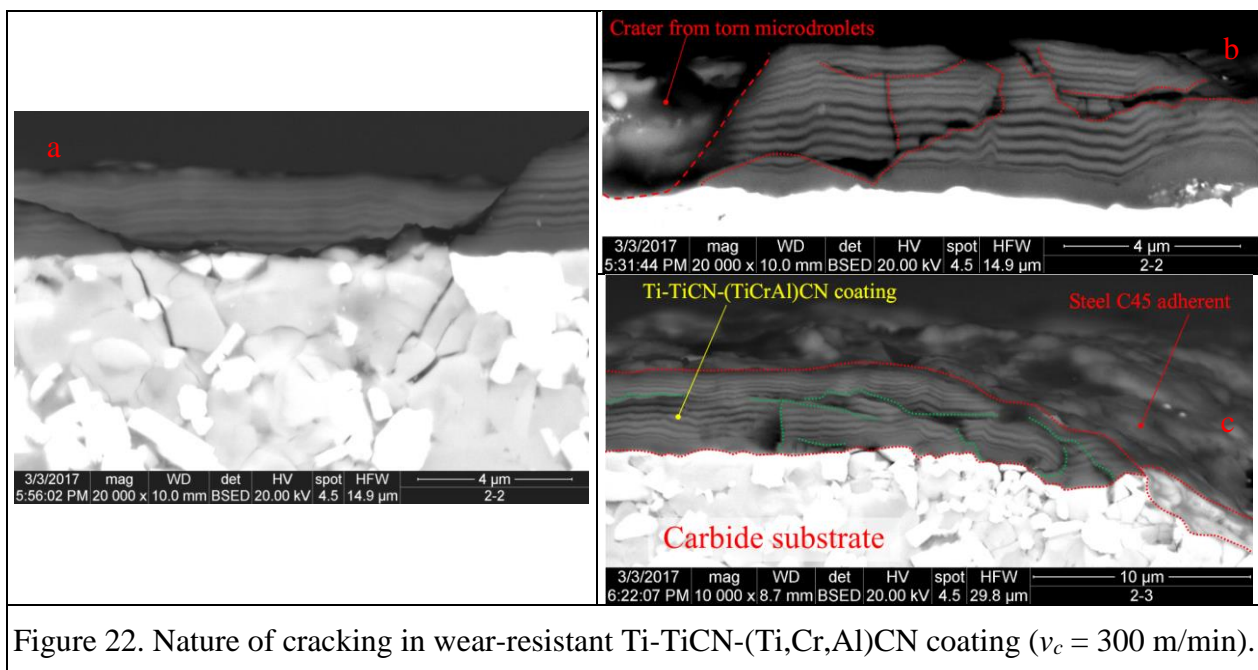


Figure 22. Nature of cracking in wear-resistant Ti-TiCN-(Ti,Cr,Al)CN coating ($v_c = 300$ m/min).

The tool flank face bear signs of brittle fracture of the substrate, manifested, among other signs, in the formation of a system of “tree-like” intercrystalline cracks (Fig. 23). Moreover, plastic micro-deformation also occurs. Meanwhile, the coating retains good adhesion to the substrate, and the nature

of its destruction resembles that of the Ti-TiCN-(Ti,Al)CN coating (see Fig. 20.a).

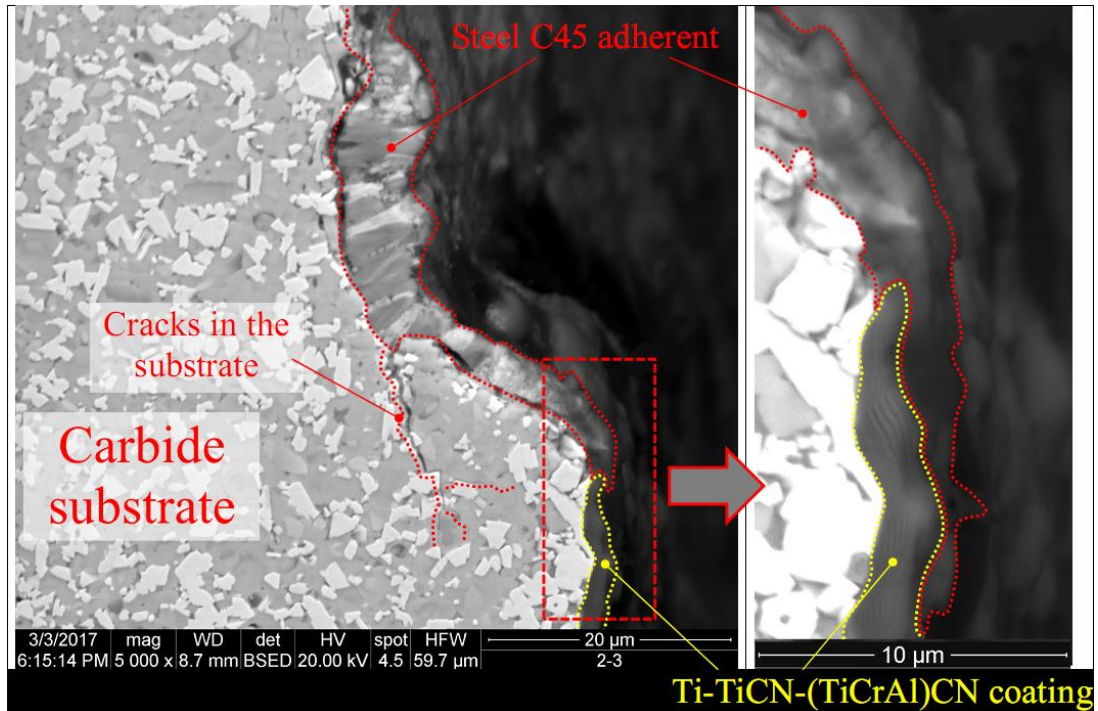


Figure 23. Nature of cracking in wear-resistant Ti-TiCN-(Ti,Cr,Al)CN coating ($v_c = 350$ m/min).

3.5. Study of diffusion mechanisms in the tool material substrate-coating system

Diffusion processes that occur during metal cutting, in particular, problems of diffusion wear, were considered in less detail than, for example, adhesion and fatigue wear or oxidation processes. It is generally believed that such processes play a secondary role in the overall picture of tool wear (except for cases of chemical affinity between the tool material and the material being machined, for example, in a case of chemical affinity between a diamond cutting tool and steel or cast iron) [42-45]. However, the study of such processes, especially for coated tools, may be of some interest from the point of view of studying the barrier functions of a coating. At first, let us consider cutting with an uncoated tool (Fig. 24). The study shows the presence of mutual diffusion between the tool material and the material being machined. A build-up of the material being machined contains tungsten (2.02 wt%) and cobalt (0.43 wt%) (Fig. 24, area 1). Meanwhile, the tool material substrate contains iron (Fig. 24, areas 2 and 3). The content of iron in the tool substrate decreases by movement from the boundary of “tool material-material being machined”, and at a distance of about 5 μm, no presence of iron is registered (Fig. 25).

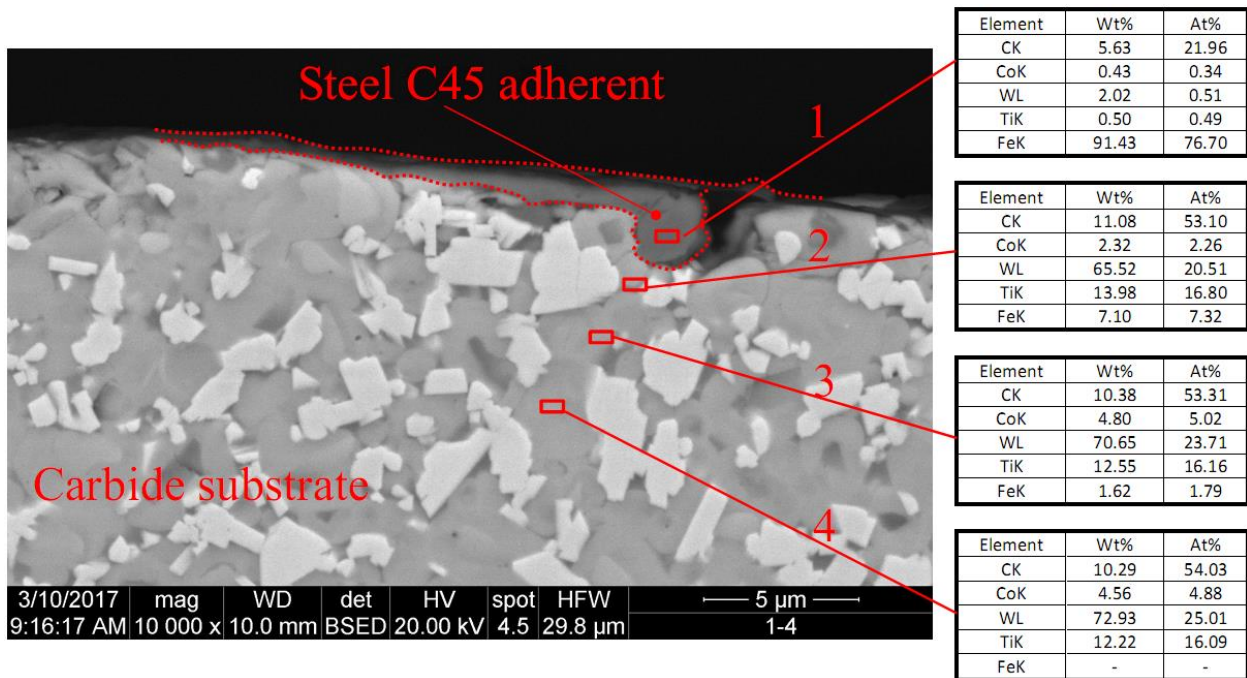


Figure 24. Diffusion processes at dry turning of steel C45 (at $a_p = 1.0$ mm; $f = 0.2$ mm/rev; $v_c = 300$ m/min) with an uncoated tool.

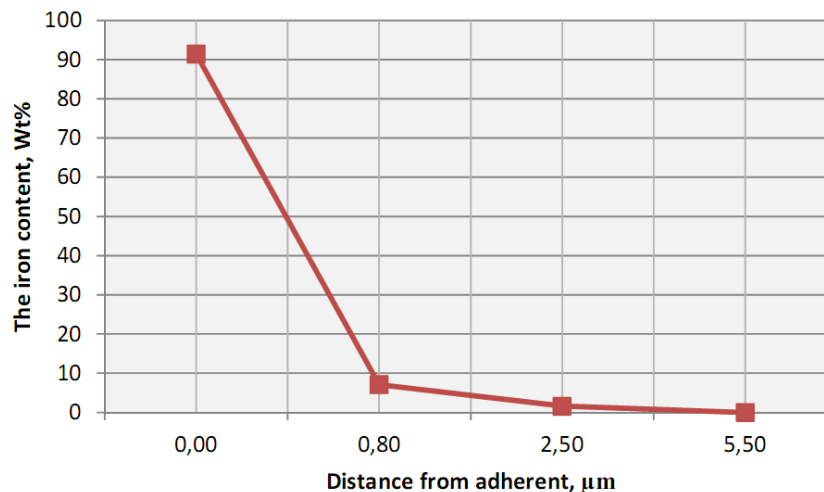


Figure 25. Change in the content of iron diffused from the material being machined in the tool substrate, depending on the distance from the boundary of material being machined.

The study of diffusion processes in a tool with a Ti-TiN coating (Fig. 26) reveals the presence of iron (2.47 wt%) and oxygen (8.34 wt%) in the surface layers of the coating (at a distance of about 300 nm from the boundary of the coating material being machined). There is also a significant content of carbon (8.17 wt%). At the same time, in the coating area, adjacent to the boundary of the substrate coating, there is a noticeable presence of tungsten (starting from 19.3 wt% in the adhesive sublayer of Ti, up to 11.54 wt% in the layer of TiN, at a distance of about 800 nm from the boundary of the

substrate coating). Diffusion of cobalt also takes place (13.62 wt% and 3.63 wt%, respectively). The extremely high content of tungsten and cobalt in the adhesion layer of Ti can be explained by the active diffusion of these elements into titanium during the deposition of a coating at high temperature (about 700°C). At the same time, an insignificant presence of nitrogen (0.96 wt%) is registered in the surface layer of the substrate (at a distance of about 500 nm from the boundary of the substrate coating).

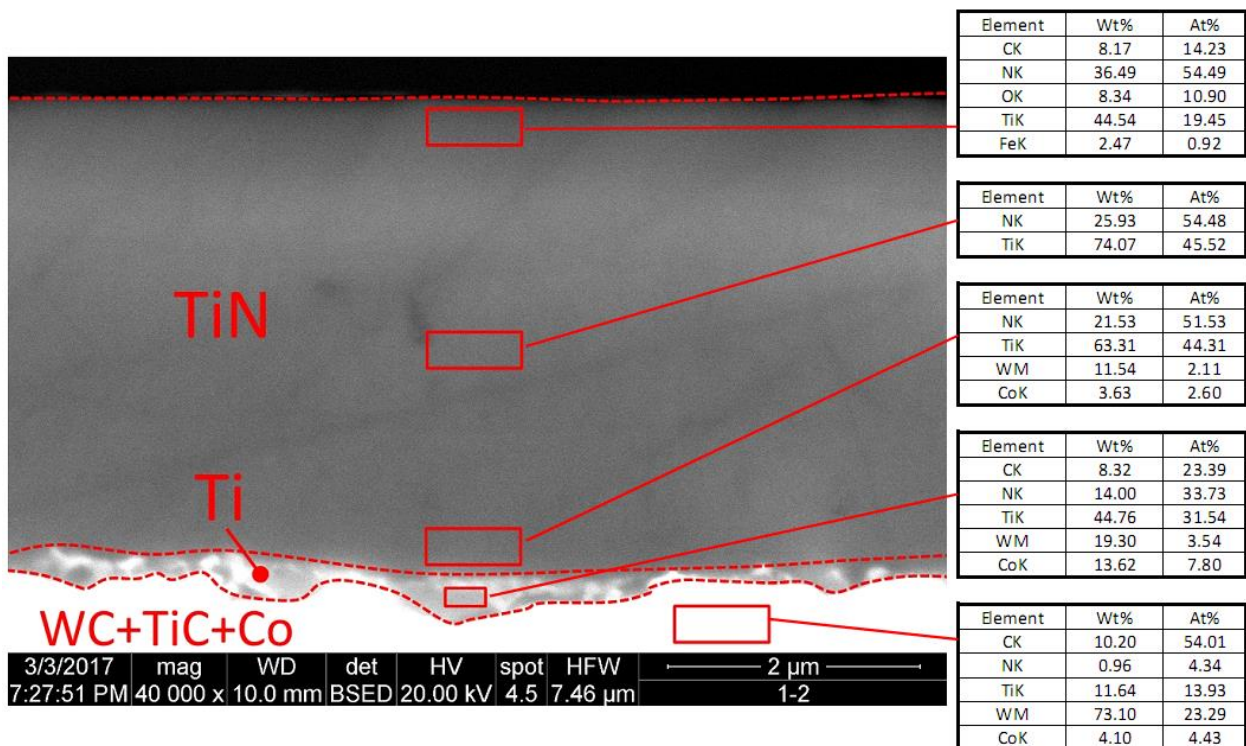


Figure 26. Diffusion processes at dry turning of steel C45 (at $a_p = 1.0$ mm; $f = 0.2$ mm/rev; $v_c = 300$ m/min) with a tool with coating Ti-TiN.

During the study of diffusion processes in a tool with multilayer nano-structured coating Ti-TiCN-(Ti,Al)CN (at a distance of about 500 nm from the boundary of the coating material being machined), there is diffusion of iron from the material being machined (0.77 wt%) and oxygen (3.77 wt%) (Fig. 27). Meanwhile, the intermediate coating layer TiCN and, in particular, the adhesive sublayer Ti show the presence of tungsten (2.60 and 27.89 wt%, respectively). The adhesive sublayer also contains cobalt (1.09 wt%).

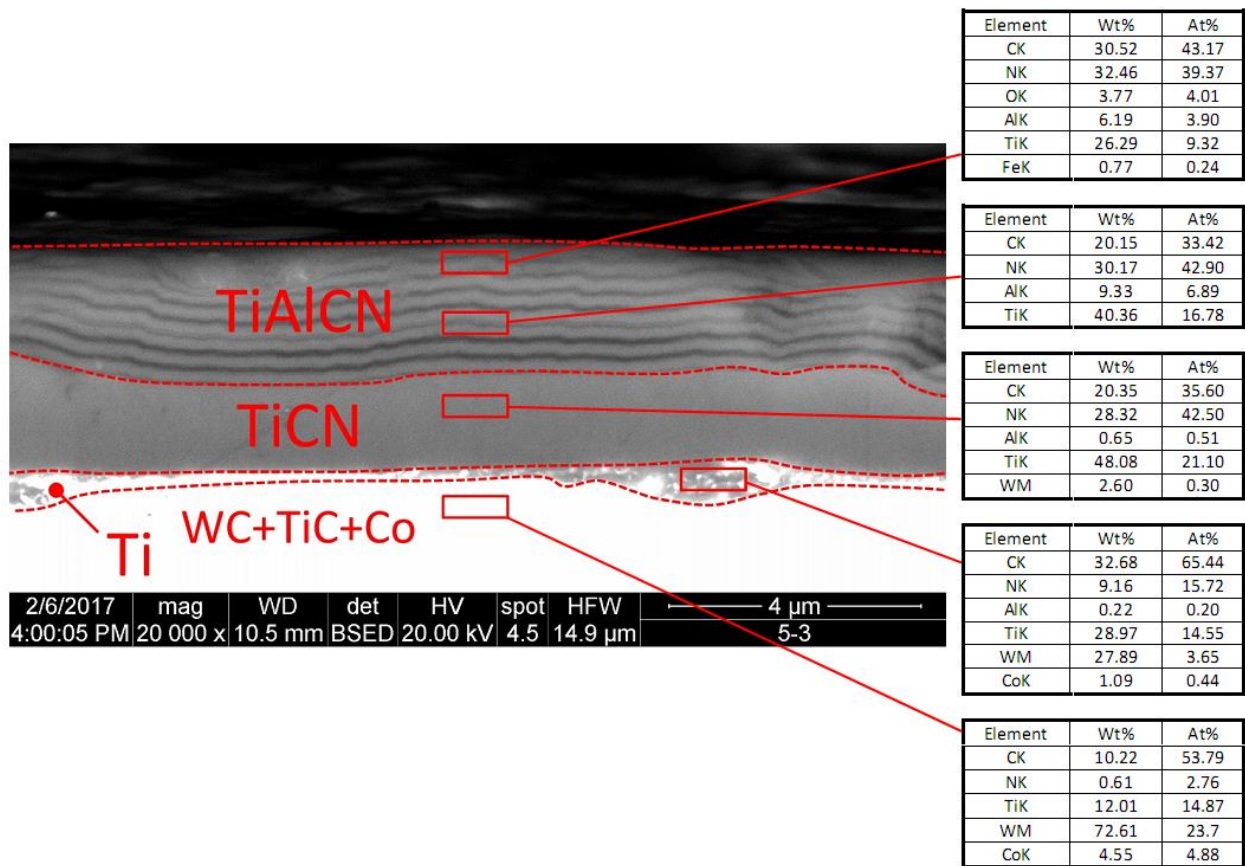


Figure 27. Diffusion processes at dry turning of steel C45 (at $a_p = 1.0$ mm; $f = 0.2$ mm/rev; $v_c = 300$ m/min) with a tool with coating Ti-TiCN-(Ti,Al)CN.

During the study of diffusion processes in a tool with coating Ti-TiCN-(Ti,Cr,Al)CN (Fig. 28), the following conclusions can be drawn.

There is an active diffusion of iron from the material being machined to a depth of 1 μm from the boundary of the coating material being machined. High content of iron (starting from 10.28 up to 13.64 wt%) is registered in the surface layers of the coating. In the area, adjacent to an embedded microdroplet, the presence of iron (6.29 wt%) is registered even in the intermediate layer of the coating, and that can be explained by active diffusion of iron on the boundary of the “microdroplet coating”. The upper layers of the coating also contain oxygen, the content of which varies significantly (starting from 0.65 up to 12.89 wt%). Active diffusion of tungsten (5.19 to 19.18 wt%) is observed in the intermediate layer of the coating, while cobalt is registered in an insignificant amount (0.38 wt%) and in one case only. Insignificant presence of nitrogen (0.61 wt%) is registered in

the surface layer of the substrate (at a distance of about 500 nm from the boundary of the coating substrate. “Contaminating” elements Si, Mg, and Ca are registered in small amounts in the surface layers. The presence of these elements is likely connected with the process of manufacturing a section.

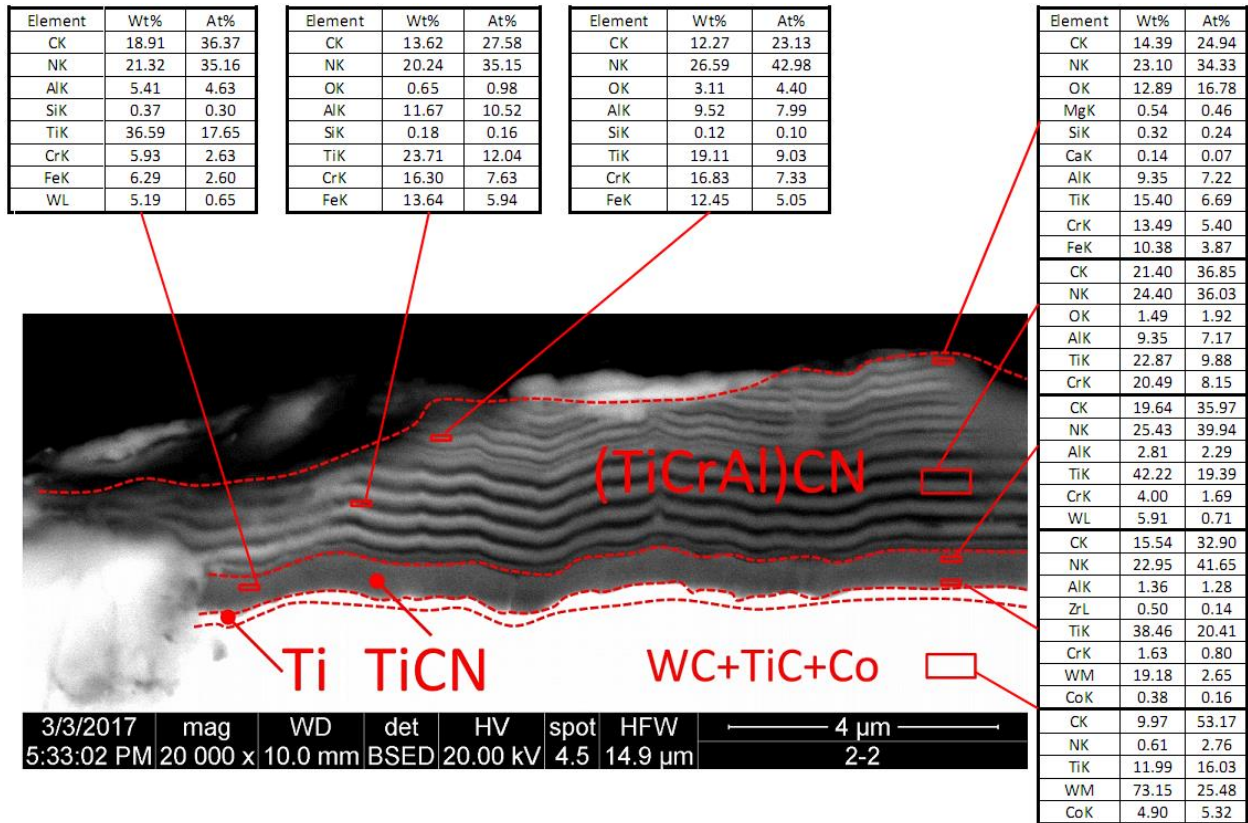


Figure 28. Diffusion processes at dry turning of steel C45 (at $a_p = 1.0$ mm; $f = 0.2$ mm/rev; $v_c = 300$ m/min) with a tool with coating Ti-TiCN-(Ti,Cr,Al)CN.

Conclusion

The study considered two multilayer nano-structured coatings based on carbonitride systems Ti-TiCN-(Ti,Al)CN and Ti-TiCN-(Ti,Cr,Al)CN. Cutting tests, in turning of steel C45 at $f = 0.25$ mm/rev, $a_p = 1.0$ mm, $v_c = 300, 350$, and 400 m/min, showed high tool life for a tool with both coatings. Meanwhile, the difference in the tool life of an uncoated tool and a tool with coating Ti-TiN, on the one hand, and the tool with the carbonitride coatings under study, on the other hand, increases with the increase in cutting speed. A tool with coating Ti-TiCN-(Ti,Al)CN showed a slightly higher tool life than a tool with Ti-TiCN-(Ti,Cr,Al)CN. As a result of consideration of the kinematics of tool wear with both

coatings, it is possible to see the balanced nature of the wear of a tool with a coating of Ti-TiCN-(Ti,Al)CN.

The analysis of the crack formation in the coatings under study has shown that the Ti-TiCN-(Ti,Cr,Al)CN coating is characterized by less crack resistance, and the brittle fracture mechanism is more typical for it, and this fact may explain the tendency to intensive wear at the final stage of operation. The analysis of diffusion processes in a tool with the coatings under study showed the following:

- presence of active diffusion of iron and oxygen from material being machined into the outer coating layer;
- presence of diffusion of tungsten and sometimes cobalt from the tool substrate into the inner coating layer; and
- presence of a barrier function in coatings, which prevents direct interdiffusion of elements between the tool material and the material being machined.

The use of the given coatings makes it possible to extend the scope of the use of carbide tools under study up to cutting speeds of 350 m/min and 400 m/min.

Acknowledgements. This study was supported by a grant of the Russian Science Foundation (theme No. 15-36 / RNF Agreement No. 15-19-00231 dated May 18, 2015).

References

- [1] K.D. Bouzakis, N. Michailidis, G. Skordaris, E. Bouzakis, D. Biermann, R. M'Saoubi, Cutting with coated tools: Coating technologies, characterization methods and performance optimization, CIRP Ann. Manuf. Technol. 61 (2012) 703–723. doi:10.1016/j.cirp.2012.05.006.
- [2] M. Tkadletz, N. Schalk, R. Daniel, J. Keckes, C. Czettl, C. Mitterer, Advanced characterization methods for wear resistant hard coatings: A review on recent progress, Surf. Coatings Technol. 285 (2016) 31–46. doi:10.1016/j.surfcoat.2015.11.016.
- [3] G.S. Fox-Rabinovich, A.I. Kovalev, M.H. Aguirre, B.D. Beake, K. Yamamoto, S.C. Veldhuis, J.L. Endrino, D.L. Wainstein, A.Y. Rashkovskiy, Design and performance of AlTiN and TiAlCrN PVD coatings for machining of hard to cut materials, Surf. Coatings Technol. 204 (2009) 489–496. doi:10.1016/j.surfcoat.2009.08.021.
- [4] Q. Yang, R. McKellar, Nanolayered CrAlTiN and multilayered CrAlTiN-AlTiN coatings for solid particle erosion protection, Tribol. Int. 83 (2015) 12–20. doi:10.1016/j.triboint.2014.11.002.

- [5] L. Bai, X. Zhu, J. Xiao, J. He, Study on thermal stability of CrTiAlN coating for dry drilling, *Surf. Coatings Technol.* 201 (2007) 5257–5260. doi:10.1016/j.surfcoat.2006.07.166.
- [6] L. Lu, Q.M. Wang, B.Z. Chen, Y.C. Ao, D.H. Yu, C.Y. Wang, S.H. Wu, K.H. Kim, Microstructure and cutting performance of CrTiAlN coating for high-speed dry milling, *Trans. Nonferrous Met. Soc. China (English Ed.)* 24 (2014) 1800–1806. doi:10.1016/S1003-6326(14)63256-8.
- [7] J.L. Endrino, G.S. Fox-Rabinovich, C. Gey, Hard AlTiN, AlCrN PVD coatings for machining of austenitic stainless steel, *Surf. Coatings Technol.* 200 (2006) 6840–6845. doi:10.1016/j.surfcoat.2005.10.030.
- [8] L. Chen, Y. Du, P.H. Mayrhofer, S.Q. Wang, J. Li, The influence of age-hardening on turning and milling performance of Ti–Al–N coated inserts, *Surf. Coatings Technol.* 202 (2008) 5158–5161. doi:10.1016/j.surfcoat.2008.05.036.
- [9] K. Yamamoto, T. Sato, K. Takahara, K. Hanaguri, Properties of (Ti,Cr,Al)N coatings with high Al content deposited by new plasma enhanced arc-cathode, *Surf. Coatings Technol.* 174–175 (2003) 620–626. doi:10.1016/S0257-8972(03)00580-2.
- [10] S. Veprek, M.J.G. Veprek-Heijman, Industrial applications of superhard nanocomposite coatings, *Surf. Coatings Technol.* 202 (2008) 5063–5073. doi:10.1016/j.surfcoat.2008.05.038.
- [11] G.S. Fox-Rabinovich, K. Yamamoto, A.I. Kovalev, S.C. Veldhuis, L. Ning, L.S. Shuster, A. Elfizy, Wear behavior of adaptive nano-multilayered TiAlCrN/NbN coatings under dry high performance machining conditions, *Surf. Coat. Technol.* 202 (2008) 2015–2022. doi:10.1016/j.surfcoat.2007.08.067
- [12] L. Ning, S.C. Veldhuis, K. Yamamoto, Investigation of wear behavior and chip formation for cutting tools with nano-multilayered TiAlCrN/NbN PVD coating, *Int. J. Mach. Tools Manuf.* 48(6) (2008) 656–665. doi:10.1016/j.ijmachtools.2007.10.021
- [13] K. Yamamoto, S. Kujime, K. Takahara, Properties of nano-multilayered hard coatings deposited by a new hybrid coating process: Combined cathodic arc and unbalanced magnetron sputtering, *Surf. Coat. Technol.* 200 (2005) 435–439. doi:10.1016/j.surfcoat.2005.02.175
- [14] S. Yang, E. Wiemann, D. Teer, The properties and performance of Cr-based multilayer nitride hard coatings using unbalanced magnetron sputtering and elemental metal targets, *Surf. Coat. Technol.* 188, (2004) 662–668. doi: 10.1016/j.surfcoat.2007.08.067
- [15] H. Ezuraa, K. Ichijoa, H. Hasegawab, K. Yamamotoc, A. Hottaa, T. Suzukia, Micro-hardness, microstructures and thermal stability of (Ti, Cr, Al, Si)N films deposited by cathodic arc method. *Vacuum* 82 (2008) 476–481.
- [16] C.-H. Lai, K.-H. Cheng, S.-J. Lin, J.-W. Yeh, Mechanical and tribological properties of multi-element (AlCrTaTiZr)N coatings. *Surf. Coat. Technol.* 202 (2008) 3732–3738.
- [17] M.G. Faga, G. Gautier, R. Calzavarini, M. Perucca, E. Aimo Boot, F. Cartasegna, L. Settineri, AlSiTiN nanocomposite coatings developed via Arc Cathodic PVD: Evaluation of wear resistance via tribological analysis and high speed machining operations. *Wear.* 263 (2007) 1306–1314.
- [18] A.A. Vereschaka, M.A. Volosova, S.N. Grigoriev, A.S. Vereschaka, Development of wear-resistant complex for high-speed steel tool when using process of combined cathodic vacuum arc deposition, in: *Procedia CIRP* 9 (2013) 8–12. doi: 10.1016/j.procir.2013.06.159

- [19] A. Vereschaka, M.A. Volosova, A.D. Batako, A.S. Vereshchaka, B.Y. Mokritskii, Development of wear-resistant coatings compounds for high-speed steel tool using a combined cathodic vacuum arc deposition, *Int. J. Adv. Manuf. Technol.* 84 (2016) 1471–1482. doi:10.1007/s00170-015-7808-5.
- [20] A.A. Vereschaka, A.S. Vereschaka, A.D. Batako, O. Kh. Hojaev, B.Y. Mokritskii, Development and research of nanostructured multilayer composite coatings for tungsten-free carbides with extended area of technological applications. *Int. J. Adv. Manuf. Technol.* 87 (2016) 3449–3457. doi:10.1007/s00170-016-8739-5
- [21] A.A. Vereshchaka, A.S. Vereshchaka, O. Mgaloblishvili, M.N. Morgan, A.D. Batako, Nano-scale multilayered-composite coatings for the cutting tools. *Int. J. Adv. Manuf. Technol.* 72(1) (2014) 303–317. doi:10.1007/s00170-014-5673-2
- [22] A.A. Vereschaka, A.S. Vereschaka, J.I. Bublikov, A.Y. Aksenenko, N.N. Sitnikov, Study of properties of nanostructured multilayer composite coatings of Ti-TiN-(TiCrAl)N and Zr-ZrN-(ZrNbCrAl)N. *J. Nano Res.* 40 (2016) 90–98. doi:10.4028/www.scientific.net/JNanoR.40.90
- [23] Y. Zeng, Y. Qiu, X. Mao, S. Tan, Z. Tan, X. Zhang, J. Chen, J. Jiang, Superhard TiAlCN coatings prepared by radio frequency magnetron sputtering, in: *Thin Solid Films*, 2015: pp. 283–288. doi:10.1016/j.tsf.2015.02.068.
- [24] S. PalDey, S.C. Deevi, Single layer and multilayer wear resistant coatings of (Ti, Al)N: A review, *Mater. Sci. Eng. A* 3 (42) (2003) 58.
- [25] X. Zhang, J.Q. Jiang, Y.Q. Zeng, J.L. Lin, F. Wang, J.J. Moore, Effect of carbon on TiAlCN coatings deposited by reactive magnetron sputtering, *Surf. Coat. Technol.* 203 (2008) 594. doi:10.1016/j.surfcoat.2008.06.175
- [26] J.M. Lackner, W. Waldhauser, R. Ebner, R.J. Bakker, T. Schoberl, B. Major, Room temperature pulsed laser deposited (Ti, Al) C_xN_{1-x} coatings—chemical, structural, mechanical and tribological properties, *Thin Solid Films* 468 (2004) 125.
- [27] J. Shieh, M.H. Hon, Plasma-enhanced chemical-vapor deposition of titanium aluminum carbonitride/amorphous-carbon nanocomposite thin films, *J. Vac. Sci. Technol. A* 20 (2002) 87.
- [28] M. Stueber, P.B. Barna, M.C. Simmonds, U. Albers, H. Leiste, C. Ziebert, H. Holleck, A. Kovács, P. Hovsepian, I. Gee, Constitution and microstructure of magnetron sputtered nanocomposite coatings in the system Ti–Al–N–C, *Thin Solid Films* 493 (2005) 104.
- [29] H.J. Choe, S.H. Kwon, J.J. Lee, Tribological properties and thermal stability of TiAlCN coatings deposited by ICP-assisted sputtering, *Surf. Coat. Technol.* 228 (2013) 282. doi:10.1016/j.surfcoat.2013.04.041
- [30] A. Köpf, J. Keckes, J. Todt, R. Pitonak, R. Weissenbacher, Nanostructured coatings for tooling applications. *Int. J. Refractory Metals and Hard Mater.* 62 (2017) 219–224.
- [31] J. Jambu, S. Latha, P. Bera, N. Hosakoppa, H. Barshilia, Optimization of process parameters to achieve spectrally selective TiAlC/TiAlCN/TiAlSiCN/TiAlSiCO/TiAlSiO high temperature solar absorber coating. *Solar Energy* 139 (2016) 58–67.
- [32] P.E. Hovsepian, A.P. Ehasarian, A. Deeming, C. Schimpf, Novel TiAlCN/VCN nanoscale multilayer PVD coatings deposited by the combined high-power impulse magnetron

- sputtering/unbalanced magnetron sputtering (HIPIMS/UBM) technology. *Vacuum*, 82 (2008) 1312-1317. doi:10.1016/j.vacuum.2008.03.064
- [33] P.E. Hovsepian, A.P. Ehiasarian, U. Rataysaki, CrAlYCN/CrCN nanoscale multilayer PVD coatings deposited by the combined High Power Impulse Magnetron Sputtering/Unbalanced Magnetron Sputtering (HIPIMS/UBM) technology. *Surf. Coat. Technol.* 203 (2009) 1237-1243. doi:10.1016/j.surfcoat.2008.10.033
- [34] K. Majid, Y. Yaghoubi, M. Eftekhari, An Analysis of TiAlCrSiCN Nanoparticles coating via PVD on Cold Work Tool Steel. *Res. J. Recent Sci.* 4 (7), (2015) 18–25.
- [35] I. Efeoglu, E. Demirci, O. Baran, Y. Totik, High Temperature Wear Resistance of TiCrAlCN/TiAlN Multilayer PVD Coatings on M2 High Speed Steel. *ICMCTF-2013 Proc.*, San Diego 2013.
- [36] A.A. Vereschaka, Development of assisted filtered cathodic vacuum arc deposition of nano-dispersed multilayer composite coatings on cutting tools. *Key Eng. Mater.* 581 (2014) 62–67. doi:10.4028/www.scientific.net/KEM.581.62
- [37] A.O. Volkhonskii, A.A. Vereshchaka, I.V. Blinkov, A.S. Vereshchaka, A.D. Batako A, Filtered cathodic vacuum Arc deposition of nano-layered composite coatings for machining hard-to-cut materials. *Int. J. Adv. Manuf. Technol.* 84 (2016) 1647–1660. doi:10.1007/s00170-015-7821-8
- [38] Alexey A. Vereschaka, Anatoly S. Vereschaka, Andre D.L. Batako, Boris J. Mokritskii, Anatoliy Y. Aksenenko, Nikolay N. Sitnikov, Improvement of structure and quality of nano-scale multilayer composite coatings, deposited by filtered cathodic vacuum arc deposition method. *Nanomater. and Nanotechnol.* 7 (2016) 1–13. doi:10.1177/1847980416680805
- [39] S.N. Grigoriev, A.A. Vereshchaka, Methodology of formation of multilayer coatings for carbide cutting tools. *Mech. & Industry.* 17 (2016) 706. doi: 10.1051/meca/2016065
- [40] W. Hume-Rothery, *Atomic Theory for Students of Metallurgy*, The Institute of Metals, London, 1969 (fifth reprint).
- [41] W C. Oliver, G. M. J. Pharr. An improved technique for determining hardness and elastic modulus using load and displacement sensing indentation. *J. Mater. Res.* 7 (1992) 1564–1583.
- [42] T.N. Loladze, Nature of Brittle Failure of Cutting. *Annals CIRP*, 24(1) (1975) 13–16.
- [43] T.N. Loladze, Strength and wear resistance of the cutting tool. *Mashinostroyeniye*, Moscow 1982 (in Russian).
- [44] T. Shibusaka, H. Hasimoto, K. Ueda, K. Iwata, Analysis of Brittle Failure of Cutting Tools Based on Fracture Mechanics, *Annals CIRP*, 32(1) (1983) 37–41.
- [45] A.S. Vereschaka, Working capacity of the cutting tool with wear resistant coatings. *Mashinostroenie*. Moscow, 1993 (in Russian).
- [46] V.P. Tabakov, The Influence of Machining Condition Forming Multilayer Coatings for Cutting Tools. *Key Eng. Mater.* 496 (2012) 80–85.
- [47] K.-D. Bouzakis, I. Mirisidis, N. Michailidis, E. Lili, A. Sampris, G. Erkens, R. Cremer, Wear of tools coated with various PVD films: Correlation with impact test results by means of FEM simulations, *Plasma Processes and Polymers* 4(3) (2007) 301–310.

- [48] M.G. Faga, G. Gautier, R. Calzavarini, M. Perucca, E.A. Boot, F. Cartasegna, L. Settineri, AlSiTiN nanocomposite coatings developed via Arc Cathodic PVD: Evaluation of wear resistance via tribological analysis and high speed machining operations. *Wear*. 263 (2007) 1306–1314. doi:10.1016/j.wear.2007.01.109
- [49] G. Skordaris, K.-D. Bouzakis, P. Charalampous, E. Bouzakis, R. Paraskevopoulou, O. Lemmer, S. Bolz, Brittleness and fatigue effect of mono- and multi-layer PVD films on the cutting performance of coated cemented carbide inserts, *CIRP Annals – Manu. Technol.* 63 (2014) 93–96.
- [50] A.A. Vereschaka, S.N. Grigoriev, Study of cracking mechanisms in multilayer composite nano-structured coatings. *Wear*. 378-379 (2017) 43–57. doi:10.1016/j.wear.2017.01.101